[redacted]

SERIAL NO. [redacted]

15 May 1945

NAVAL RESEARCH LABORATORY
WASHINGTON 20, D. C.

BEND TESTING AT BALLISTIC SPEEDS.
FIRST PARTIAL REPORT:
TECHNIQUE AND SURVEY OF TYPICAL RESULTS

BY
HERSCHEL L. SMITH
and
ARTHUR E. RUARK

Me h. & Elec. Division - Ballistics Sec.

Report No. 0-2531; Problem No. 0-46

[redacted]

FR-2531

Approved by
A.V.H. Masket,
Acting Head, Ballistics Section

Dr. Ross Gunn, Superintendent,
Mechanics & Electricity Division

A. H. Van Keuren, Rear Admiral, USN
Director, Naval Research Laboratory

Title Page
Abstract
Table of Contents
Text - - - - 25 Pages
Figures - - 20 Pages

[redacted]

[redacted]

DECLASSIFIED

35 - Metallurgy

15 May 1945

[redacted] 35

NAVAL RESEARCH LABORATORY
WASHINGTON 20, D. C.

CLASSIFICATION CANCELLED OR CHANGED
TO Unclassified
BY AUTHORITY OF DOD DIR. 5200.9
ON
SIGNATURE

6214

BEND TESTING AT BALLISTIC SPEEDS. FIRST PARTIAL REPORT: TECHNIQUE AND SURVEY OF TYPICAL RESULTS

BY
HERSCHEL L. SMITH
and
ARTHUR E. RUARK

Mech. & Elec. Division - Ballistics Sec.

Report No. 0-2531; Problem No. 0-46

[redacted]

Approved by
A.V.H. Masket,
Acting Head, Ballistics Section

Dr. Ross Gunn, Superintendent,
Mechanics & Electricity Division

A. H. Van Keuren, Rear Admiral, USN
Director, Naval Research Laboratory

Title Page
Abstract
Table of Contents
Text - - - - 25 Pages
Figures - - 20 Pages

DECLASSIFIED

ABSTRACT

High velocity bend tests have been carried out at NRL for some time by bullet impact on notched specimens, which are mounted on a ballistic pendulum to measure the bullet velocity.

Very high strain rates, of the order of 10,000 inches per inch per second, can be achieved in this test. The technique has been improved steadily and present practice is clearly indicated by the Figures, showing apparatus and specimens.

Section I deals with the propagation of stress and strain through specimens which are subjected to impact, and summarizes previous work.

Section II describes technique.

Section III shows the types of results which have been obtained. The test has been used in comparisons of the efficiency of welded joints, in the development of experimental armor steels, and in the study of temper brittleness and allied phenomena in heavy armor. Comparisons of the performance of magnesium and aluminum alloys under this high speed test are contained in a companion report, NRL No. 0-2532.

In Section IV the dynamical basis of the test is discussed and side experiments on bullet rebound and on fragments thrown from the specimen face are presented.

Appendix I contains a more detailed discussion of the propagation of stress and strain in bodies subjected to shock.

[redacted]

TABLE OF CONTENTS

[redacted]

DECLASSIFIED

TABLE OF CONTENTS Cont'd

DECLASSIFIED

[redacted]

DECLASSIFIED

INTRODUCTION I

A. Authorization

1. This work was authorized as follows:

BuOrd Project No. 40025, 8 July 1944.
BuAer Project No. 83/45, 17 July 1944.

B. Previous Work

2. In recent years the study of the dynamic properties of metals has undergone much development along five related lines.

(a) A theory proposed by von Karman and G. I. Taylor has given us a clear understanding of the way in which plastic deformation spreads out from a region subjected to sudden impact, although only a few simple cases have been worked out in full detail.

(b) This theory has been verified by special tests on wires, and tensile impact experiments have been carried out on many metals and alloys (Refs. 2-5 and 13).

(c) A few investigators have concerned themselves with compression tests at high speed (Ref. 8).

(d) The plastic bending of beams and plates under impact has been studied (Ref. 3).

(e) Investigators too numerous to mention have made observations of the change from ductile to brittle fracture in steels, working usually at the speed of the customary Izod and Charpy machines, that is, at impact-speeds of 10-20 feet per second. A great deal of attention has been devoted to the effect of low temperature in promoting brittle fracture (Ref. 11).

3. The destruction of a plate or any other structure by a projectile or a shock wave involves complicated distributions of stress and strain. The general objective of workers in this field is to study the plastic flow and the phenomena of fracture under simple stress distributions. As the rate of loading increases, it becomes more difficult to measure the strain rate at any particular point in the specimen, because of the finite speed with which stress and strain are propagated from the place where the load is applied. Each increment of stress or strain moves with a different velocity. Reflection of both the plastic and the elastic waves of deformation still further complicates the picture.

4. The consideration of these waves is necessary for a complete understanding of any impact phenomenon. However, in the present report we shall dispense with such a complete understanding. Our goal in the

DECLASSIFIED

experiments described here was to compare the energies required to rupture bend specimens at high speed. In interpreting such comparative tests a simpler treatment suffices for present purposes. For the sake of completeness, we include a survey of plastic wave phenomena in the Appendix. Here it will suffice to outline only the most general results of previous work without attention to many refinements.

5. First we must state the strain rates employed in previous investigations. The rates are expressed in inches per inch per second, which will be written as "per second" hereafter, since strain is a dimensionless number. With one exception (Ref. 5), in which strain rates as high as 16000/sec have been secured in a notched tensile specimen, the existing body of published work on tensile and compressive impact tests has been done at strain rates less than 2000/sec. In fact the average rate is only a few hundred per sec. in the extensive body of work done at the California Institute of Technology (Refs. 2,3), to which we now turn our attention.

6. <u>California Institute Tests.</u> The California investigators have emphasized difficulty of determining strain rates, caused by the propagation of the strains. However, if the specimen length is L, a conventional strain rate de/dt can be calculated from the impact speed v by means of the relation $de/dt = v/L$. This quantity is useful for comparative purposes. In much of the work at the California Institute of Technology specimens 0.67 ft. long have been employed. Thus the strain rate in these experiments is $v/0.67$ when v is expressed in fps. The velocity goes up to about 200 fps in most of the work; the corresponding strain rate covers the approximate range 25-300/sec., and the general findings are as follows:

(a) The tensile strength generally rises in the domain of impact speeds from 0 to 25 fps. The rise varies from zero to 50 per cent. Beyond this speed, the tensile strength remains constant, up to about 200 fps, and beyond that speed little is known about it.

(b) The elongation rises, only to drop again when the so-called critical velocity is reached. At this velocity, the stress at the region where force is applied is equal to the tensile strength. Under such a stress the metal must neck and rupture locally, and the general elongation of the remainder of the specimen is suppressed as compared with the value obtained in static tests or at much lower velocities. The drop of the elongation from its maximum value may be enormous, --65 to 70 per cent.

(c) Thus, changes of elongation are usually the dominating factor in determining the ratio of impact work and static work, though the influence of change in the stress at given strain is by no means negligible. In ductile metals, the work usually rises initially because of increases of both the strength level and the elongation, only to fall again when the elongation experiences its decrease. Often this

[redacted]

occurs at speeds of 80-150 fps, or strain rates of 120-225/sec., in the California Institute tensile impact tests.

(d) It is not always clear that the drop in elongation arises from exceeding the critical velocity. There are sometimes marked discrepencies between the experimental and the calculated values of the speed at which the drop occurs. These troubles may be due to the effect of strain-rate on the general course of the stress-strain curve; to a change from ductile to brittle fracture; or to both causes. The missing link in many tensile impact investigations is the absence of recorded data on the reduction of area and on changes of fracture type, especially in the case of steels at hardness levels which might be expected to lead to brittle fracture. The lack of test results at sub-room temperatures also hampers the interpretation of results.

(e) However, we have found a reasonable way to judge whether the drop in elongation is accompanied by a change in the detailed mode of fracture. In the case of the California Institute data, reduction of area is customarily given, and if it does not decrease when the velocity increases and the elongation falls, we can feel fairly confident that no change from ductile-type fracture to cleavage fracture has occurred.

7. Need for Tests at Higher Strain Rates. It must be noted that the strain rates so far achieved in tensile impact tests on unnotched specimens are no higher than those obtained in routine impact tests using the customary specimen with the Izod V-notch. (See the Appendix for details.) Our own work is motivated by the desire to make tests at strain rates of the magnitude met with in the penetration of plates by service projectiles.

C. Statement of Problems and Outline of Work Done

8. The problems attacked are as follows:

(1) Development of a bend test in which one part of a notched specimen is separated from the other part by bullet impact. The specimen is mounted in a ballistic pendulum so that the energy can be measured. The lines of attack were determined to a large extent by the applications found for the test, namely, (a) study of the rupture energy of welded and unwelded specimens; (b) study of both experimental and convential armor steels, and (c) measurement of the high-speed-bend behavior of 16 commercial magnesium alloys and several commercial aluminum alloys.

(2) Development of methods for inferring the fraction of the total energy which is devoted to the task of breaking the specimen at the notch.

9. Work on the development of the test is described in Section II. Extensive work has been done on application (a) in cooperation with the Welding Section, Division of Physical Metallurgy. (Refs. 18-21 and

[redacted]

DECLASSIFIED

Section III-A of this report. The test has been applied to experimental armor steels of the high manganese, low nickel type at the request of the Special Alloys Section, Division of Physical Metallurgy, which developed these steels. The effects of varying alloy content and of diversified heat treatments were tested. (Refs. 22-23 and Section III-B of this report.) Also the method was used to reveal the presence of temper brittleness in specimens of 18" armor plate, (Section III-C). In one particular case, the temper brittleness was not detectable by slow bend tests or Charpy impact tests.

10. Finally, the method was applied to a number of magnesium and aluminum alloys. This work is described in Ref. 16. As to problem 2, a complete interpretation requires a knowledge of the variation of force during the bullet impact, and as indicated above, a knowledge of the plastic-wave propagation in the specimen. We content ourselves for the present with an approximate treatment which suffices only for the purpose of comparing specimens which are not too dissimilar in their properties. Currently the test is being employed to extend our knowledge of the effect of strain rate and of size on the rupture work of steels. As pointed out above, the strain rates attained in previous experiments are for the most part lower than 2000/sec., while the present test makes it possible to achieve rates of the order of 10,000/sec. with relative ease. It is hoped that comparison of the data with those from slow bend tests or standard impact tests will yield useful information about the variation of energy consumption with strain rate.

EXPERIMENTAL METHODS II

A. General Description of the Facilities and the Method

11. Figures 1 - 4 show a smooth bore 50 caliber gun with silencer, arranged to fire into a 450-pound ballistic pendulum. Figure 5 is a side view of the pendulum with its removable cover raised by a hoist so that the reader may observe a specimen mounted in a suitable steel jig in the path of the projectile. The same jig and specimen are shown, in closer view, in Figure 9, together with two of the special types of ammunition employed. Various specimen types, shot and unshot, may be seen in Figures 11, 13, and 14. The bullet velocity required to rupture specimens of a given metal is directly measured by the ballistic pendulum, since all parts inside the case come to rest, relative to the pendulum, in a time short compared with its period of swing. The energy imparted to the specimen and its high-inertia mounting depends on the rebound velocity of the bullet as well as its initial velocity. Some experiments have been made under representative conditions to determine the energy-correction for rebound. Fortunately it is less than one per cent in the worst case and usually is only 2 or 3 tenths of one per cent.

12. Roughly speaking, the bullet energy is divided into a part E_b which produces plastic flow at the place of impact, a part E_w which escapes to the mounting in the form of elastic wave energy, and a part E_n which serves to separate the specimen at its notched section. To a first approximation, if the specimen is treated as a rigid uniform bar, struck at its center of percussion, the fraction of the bullet energy is employed at the notch is

$$E_n/(\tfrac{1}{2}mv^2) \cong 1.33m/M \qquad (1)$$

where m is the bullet mass and M the specimen mass. Section IV may be consulted for a more accurate formula. It turns out that an accurate determination of E_n would involve a knowledge of the rebound velocity, the angular momentum of the rebounding projectile, and the torque-time curve for the material at the notch. It is not practical at present to take all these factors into account, so a very simple equation (eq. 6 in Section IV-B) is used for calculating comparative values of E_n for similar specimens. Efficient transfer of energy to the notch requires a high value of the ratio m/M. In much of the work described in this report the advantage of high utilization was sacrificed in order to make use of easily available steel spheres as ammunition. Recently, however, we have made special hardened projectiles in the form of long cylinders with hemispherical ends. These are now used in most of our work. The m/M value is limited to about 0.44, to avoid excessive follow-through. Even with this m/M value, the projectile may continue to travel forward in some cases. When this happens it strikes the specimen additional weak blows as the latter slows down.

13. It will be well to compare this equipment with high speed impact devices which have been used elsewhere. The prevailing type described by recent investigators (Refs. 2, 4, 6, 8) consists of a

[redacted]

massive wheel which is able to set one end of a specimen in motion with a speed of the order of 200 fps, without substantial decrease of velocity during the process. Energies of the order of 10,000 ft. lbs. can be delivered to the specimen. Our apparatus has a nominal advantage as far as impact velocity is concerned. The pendulum measures bullet velocities from 500 to 3000 fps with ease, using conventional projectiles, and the lower end of this range can be extended by using special ones. Energies of the order of 14,000 ft. lbs. can be delivered to the specimen if necessary though we prefer to use smaller energies by properly matching the projectile mass to that of the specimen. The velocity during impact is not constant, and the angular velocity of the bend specimen decreases as it bends. Similar remarks would apply if the machine were employed as a tensile impact tester. These circumstances are deemed relatively unimportant for the apparatus has proved to be convenient, rapid, and flexible in tests on a variety of materials. We turn now to more detailed descriptions.

B. <u>The Gun and the Ballistic Pendulum</u>

14. Figure 2 portrays a smooth-bore 50 caliber gun and its recoil devices, mounted on machined sliding ways which insure constant alignment. The firing device is not shown. It is actuated by air pressure from a station outside the armored laboratory room. Figure 3 shows a very effective silencer. The noise from this gun is not in any way objectionable. While the silencer takes care of most of the blast, it is still further reduced by shooting through a 1/8" rubber sheet, held in a circular clamp which is seen at the center of the silencer, in Figure 4.

15. The pendulum, Figures 4-6, is built on the general principles described in Ref. 24. These figures demonstrate the accessibility of the interior, the cover being raised by an electric hoist. Adjustable suspension wires are clearly visible. After initial alignment, adjustments are infrequent. Duct systems are provided to remove combustion products from the silencer and the pendulum. After a deflection, the pendulum returns to the right and is checked by coming into contact with a sloping surface on the duct, shown below the right end of the pendulum. Slots in the pendulum base then permit quick exhaustion of vapors and dust.

16. Figure 7 shows a simple and accurate pulley-and-weight device for calibrating the pendulum. The deflection recorder, Figures 7 and 8, consist of a fixed scale, and a slider which moves with negligible friction and negligible overthrow along this scale, when pushed by a pair of fingers attached to the pendulum.

17. Momentum is imparted along a line close to the center of gravity of the pendulum. Because of projectile rebound and specimen motion, complete momentum transfer takes a finite time, and therefore the pendulum measurement is slightly low. However, considering all errors of the pendulum, an accuracy of 1/2 per cent, or better, is customarily attained in the momentum measurement; of course the figure would rise if we dealt with very small moments.

18. A variety of jigs and specimen-holding devices can be put in place and firmly held with simplicity and speed. Typical jigs and projectiles are shown in Figures 9 and 10. Usually the jig weighs about

60 times as much as the specimen, so constraint is effectively supplied by inertia. The specimens are mounted in such a way that plastic flow in the region of the notch is not constrained by the jig. For example, in the jig of Figure 9, which shows the back side, a 1/4" radius is cut at the top of the back support, just below the bottom of the holes in the specimen. Customarily, the muzzle is about 27" from the specimen, the gun being aimed at the center of percussion of the part of the specimen above the notch.

C. Specimens and Projectiles

19. Specimen shapes of considerable variety have been employed, depending on the purpose of the test.

20. Welded Specimens Figure 11 portrays specimens in which notch action is provided by a welded section. These make possible a rapid quantitative test for development studies of the welding of armor. The specimens are usually 1" thick, consisting of a heavy base 2-1/2" x 5" with 3 fingers extending from one side. The fingers are 2-1/2" long and 1" wide with a clearance of 1/2" between fingers and 1/2" on each shoulder to provide reasonable similar stress patterns for all fingers. They are knocked off with 0.50-caliber ball projectiles, shot backwards. Since the bullet core is fairly soft, it mushrooms considerably, and a great amount of kinetic energy can thus be delivered with only a small amount of penetration. Tests are performed on whole armor and then on single-V or double-V welded armor and efficiency of the weld under high-speed deformation is thus determined.

21. For work of this type carried on in the past no correction has been made for the energy of the rebounding projectile. A close examination of the fired projectile and the inside of the mounting jig, showed that this rebound energy is small. The energy transfer factor is about 0.25 and the limit velocities are usually from 1700 to 2300 ft/sec. The test is used only for comparative purposes.

22. Notched Steel Specimens Similar remarks apply to the notched armor specimens shown in Figure 13.

23. Magnesium and Aluminum Alloy Specimens Three specimen types were employed in the course of our study (Ref.16). Figures 14 and 15 show specimens and fractured surfaces. The simple notched type is preferred whenever it can be used. The notch of 1/8" root diameter and 3/16" depth is a more severe stress raiser than the holes (0.187" diameter) in the drilled type. Part of our work (Ref.16) consisted in the comparison of rolled and extruded bars and it was desirable to retain as much as possible of the surface metal on the front and back of the specimen. Hence the hole type of specimen was employed; it leaves 3.38" of the perimeter intact while the figure is only 2.62" for the notched specimen.

[redacted]

24. We first present a few results selected from earlier reports on armor steels, the purpose being to give some idea of the range of problems which can be attacked. The results of an extensive investigation of magnesium alloys are presented in a companion report, (Ref.16).

A. Tests on Welded and Unwelded Samples of Armor Steel

25. A variety of tests have been made for the Welding Section, Division of Physical Metallurgy (Refs. 18-21). As an illustration, attention is called to Figure 12. A laboratory test was desired which would give an indication of the crack-susceptibility of welded armor plates. A standard test for this is the H-plate test, in which several rectangular pieces are joined so that the welds form a letter "H". The plate is attacked at normal incidence with projectiles of suitable diameters. Figure 12, from Ref. 18, shows the correlation of limit-velocity for the rupture of the specimen type shown in Figure 11, with the results of H tests of the same plates. Here the criterion employed for measuring damage in the H test is the total length of the cracks in the leg joints of the H, no matter whether there be one crack or more than one.

26. Reference 19 gives comparisons of the performance of unwelded specimens of low-alloy ballistic steels with that of special treatment steel. The joint efficiencies of single vee butt welds made from these steels were determined, and studies of electrode materials were carried out, by means of the ballistic bend test. Reference 20 carries the studies further for semi-restrained double vee weldments and restrained single vee weldments, while Reference 21 is an investigation of Unionmelt welding of STS armor.

B. Tests on Iron-Manganese and Iron-Manganese-Nickel Alloys

27. The Special Alloys Section of NRL has developed an interesting class of alloy steels containing roughly 4% manganese, or manganese, nickel and other elements (Refs. 22, 23). These alloys possess a very valuable property, namely, temperature of the transformation from gamma to alpha is not affected by the rate of cooling. This statement holds true down to cooling rates of the order of magnitude encountered when an 18" plate is cooled in air. Further, this transformation temperature is lowered so that a martensitic structure is produced throughout a large section on slow cooling. This means that after slow cooling and tempering such alloys, it is possible to have ductility equal to or superior to that of a fully quenched and tempered steel. Some of the alloys show low temperature impact properties superior to those of STS deck armor, in comparable thicknesses. For example, in one case (heat MDS, Ref. 22), the Charpy V-notch work value is about 112 ft. lbs. at -60°C while a sample of STS deck armor gave 82 ft. lbs. at the same temperature. The ductile-brittle transition range for both lies below this temperature, being at a lower temperature for heat MDS than for the STS deck armor. Some of the alloys can be made to give high values of the ratio of yield strnegth to tensile strength.

28. Throughout these investigations, the ballistic bend test has been used, at room temperature and also at sub room temperatures, to measure the crack resistance of these alloys under high strain rates. The more important features are as follows:

(a) The specimen type for this work is shown in Figure 13. The fingers are 1.5" wide, 1.25" thick and are notched to a depth of 0.375", with a 1/8" circular root diameter.

(b) In order to have comparisons with other materials, specimens were made from 1.75" STS deck armor and from the center portions of a 12" Carnegie-Illinois plate (DD804) and an 18" Bethlehem plate (4A443A1).

(c) The ductile brittle transition was investigated at ballistic speed for a deck armor STS-D2 and an alloy which, with closely related ones, has received special study because of its desirable combination of properties. The analysis shows 3.52% Mn, 1.53% Ni, 0.47% Mo, 0.25% Si, and 0.14% C. The results are portrayed in Figure 20. It is seen that although the transition range commences at a higher temperature for this alloy than for STS-D2, the former shows higher test values than the latter at all temperatures employed.

(d) In most of the alloys studied, quenching from the temper leads to higher limit velocities than air cooling after the temper. However, this is not true of MKS, which yielded the very high limit of 3600 fps in both conditions, after a tempering treatment at 1112°F for 4 hours, the final hardness being 239 BHN. This figure is 13% higher than the value for a certain batch of STS at the same hardness; that is to say, the bullet energy required is 28% greater. Caution should be exercised in interpreting results of this kind; it is not implied that the limit would be 28% higher in a conventional limit velocity test. This is clearly shown by the fact that the bend test limit velocities drop off with increase of hardness in the range in 200-290 BHN, while the reverse would be the case for penetration-limits of plates having the same thickness. This simply means that the resistance of these steels to crack formation and propagation decreases as the BHN goes up, which is the expected behavior. It is reasonable to expect that the bend test will correlate well with back-of-plate cracking in ballistic limit tests with non-deforming projectiles, but this remains to be established by experiments.

C. <u>Study of Brittleness Factors in Heavy Armor</u>

29. At the request of the Special Alloys Section, the high speed bend test was employed to give evidence of the existence of temper

brittleness in an 18" Bethlehem plate, (4A443A1). Specimens were cut at points extending from the plate face to the center, and were tested at room temperature. Roughly it can be said that starting at the plate face the first two specimens lay in martensite while the remainder were situated in bainite. After initial tests in the as-received condition, a similar series of specimens were retempered and quenched. The properties were considerably improved, as judged by test results after correction for the inevitable hardness changes. Next a similar series was completely reheat-treated; all of the specimens were then martensitic. As expected there was a further improvement in the performance of the specimens which had been bainitic.

30. The significant point about these tests is that the temper brittleness in the plate interior which they reveal so clearly was not detectable in room-temperature Charpy V-notch tests and slow bend tests. The deleterious influence of the slow cooling of the plate interior is definitely dependent on the strain rate. These matters will be discussed in detail in a forthcoming report by the Special Alloys Section. (Ref.26)

[redacted]

A. Estimate of Strain Velocity in the Ballistic Bend Test

31. We require only a rough estimate, or a conventional measure, of the strain velocity during plastic bending of the specimen, so let us suppose that all the flow occurs in a region of length 2X, equal to the root diameter of the notch. Since we are interested only in relative strain rates, we neglect the presence of the notch, and consider the idealized specimen in Figure 17. This shows the specimen in the initial condition, and also after the region 2X has bent uniformly, the total bend angle being θ. It is seen that roughly

$$e = \frac{D}{X}\,\frac{\theta}{4}\,.$$

The point of application of the deforming force has moved a distance $S = L_p\theta$, at a velocity V, so $e = DS/4XL_p$, and the strain rate is

$$\dot{e} = \frac{V}{4L_p}\,\frac{D}{X} \qquad (1)$$

Two specimens shot at the same velocity and having the same conventional strain rate as given by Eq. (1), may not actually have the same strain rate. The rate will be higher for the more brittle specimen. The reader will understand that the rates discussed are those occurring before cracking takes place. In the immediate neighborhood of an advancing crack head the concept of strain rate loses its usual meaning because we have to pay attention to the displacements of individual atoms as they lose contact with each other. We can easily make estimates of a quantity which may be called the "atomic strain rate". If the bond between two atoms breaks and each one moves a distance y in time t to reach a new condition of equilibrium, then the atomic strain rate would naturally be defined as y/at, where a is the lattice spacing. This strain rate is of the order of 10^{12}/sec., a figure which helps us to understand that the properties of cracking metal may be entirely different from those possessed by the same piece before the onset of cracking.

32. For one of our specimen-types, the one provided with bored holes, $D = 0.75"$. X may be taken as equal to the hole-diameter, 3/16", and $L_p = 0.109'$. On this basis, the conventional strain rate is

$$\dot{e} = 9.2V,$$

with V in feet per second. For a specimen with a face-notch 3/16" deep and 1/8" wide, this is replaced by $\dot{e}_c = 10.3V$, if we take $D = 9/16"$ and $X = 1/8"$.

33. In our tests on magnesium and aluminum, for a bullet speed of 1000 fps, V is of the order of 160 fps and $\dot{e}$ is about 1600/sec. These values can be greatly increased by using sharper notches and smaller values of D, as we have done in some experiments on steel which will be reported elsewhere. In one of these tests we have approximately the following conditions:

[redacted]

$$\dot{e} = \frac{D\,V}{4X\,L_p} = \frac{0.47'' \times 254 \text{ fps}}{4 \times .020'' \times 0.109 \text{ ft.}} = 13700/\text{sec.}$$

The possibilities of further increase are not exhausted. For comparison, we may mention that the highest plastic strain rates we have found in the literature are approximately as follows:

In tensile impact test (Ref. 5): 16000/sec.
In compression impact tests (Ref. 8): 1600/sec.

To supply another comparison we estimate that when a 1/2" plate is struck by a 50 caliber bullet having a blunt ogive, at about 1400 fps, the average shear-strain rate in material within one-half caliber from the bullet hole may be as high as 30,000/sec.

34. It is apparent that ballistic bend experiments of the kind reported here are well adapted to improve our information in the region of relative ignorance which extends from about 300/sec to the strain rates encountered in conventional bullet tests. The difficulty with plate-and-bullet tests is the complication of the stress and strain patterns, and the accompanying lack of control of strain speed. A real advantage of the ballistic bend test is the degree of control over these factors which it provides.

B. Dynamics of the Ballistic Bend Test

35. General Description Referring to Figure 16, let a bullet strike the specimen. The following symbols will be used, with primed quantities referring to conditions after the impact:

- m, M; masses of the bullet and of the part of the specimen above the notch.
- v; initial velocity of the bullet, directed along the x axis.
- v'_x, v'_y; x and y components of the final velocity of the bullet.
- V'; velocity of the center of gravity of the specimen at the termination of the impact.
- w, w'; initial and final angular velocities of the bullet around an axis perpendicular to the plane of the paper. Other components will be neglected for simplicity.
- ω'; final angular velocity of the specimen.
- i; moment of inertia of bullet about its center of gravity, around an axis perpendicular to the paper in Figure 16. This is $0.4mr^2$ for a sphere.
- I; moment of inertia of specimen around axis 0 at the notch. Neglecting material removed at the notch, this is $M(L^2/3 + D^2/12)$ for a rectangular specimen.
- x, y; position of center of gravity of bullet at instant of impact, relative to axis 0. If the bullet strikes at the center of percussion, $y = I/Mz$.
- x', y'; similar quantities at the end of impact.
- z; distance from 0 to center of gravity of the specimen.
- E; energy utilized in plastic deformation and creation of elastic waves. This symbol is provided with suitable subscripts to indicate the location of the energy involved.

Let us review the sequence of events without regard to refinements. We assume for the moment that the bullet makes its imprint instantaneously, without delivering any kinetic energy to the pendulum. Its kinetic energy is used up in the following ways. An amount E_b is used to dig the bullet hole and to create elastic waves in the specimen. Waves in the air can be neglected. The specimen commences rotation, substantially about axis 0, with kinetic energy $1/2\ I\ \omega'^2$, and the bullet rebounds with velocity components v' and v", and angular velocity w'. If m/M is relatively large, v' may be positive, that is, directed toward the right in Figure 16. (The case in which the bullet sticks in the specimen does not require separate consideration, for in this case we simply put

$v' = V'\ (y/2),\ v'' \cong 0,\ w' = \omega'$). Momentarily, the pendulum does not receive any appreciable momentum from the specimen, because care is taken to hit the specimen at or near its center of percussion, so that no shear forces are present at the level of the notch. Let us consider the physics involved. The specimen is hit above its center of gravity, which moves to the right in accordance with the principle of momentum conservation. At the same time, it rotates clockwise so that the backward motion of the bottom due to the rotation is just cancelled by the forward translation of the whole body. In the idealized case under consideration, we shall assume that the bending moment at the notch is very small during the bullet impact since the specimen has barely begun to bend. In actuality, this assumption is rough and can lead to considerable error; it is abandoned further on.

36. In the next stage, after impact is completed, the specimen exerts a bending moment on the pendulum and transfers its forward momentum to the pendulum. Since the pendulum mass is about 4000 times the mass of the specimen, its kinetic energy is negligible compared with the bullet energy. Practically all of the kinetic energy of the specimen is used to supply an energy, E_n, to the metal in the neighborhood of the notch and to create elastic waves of energy E_w in the apparatus. Therefore the energy equation is

$$mv^2/2 = E_b + E_n + E_w + m(v'^2 + v_y'^2)/2 + iw'^2/2 \qquad (2)$$

The pendulum measures mv directly, after all parts inside it have ceased to move about.

37. From these remarks it might be thought that the ballistic bend test is merely a measure of the work required for partial penetration of the specimen, plus a method for producing a rapid fracture by means of stresses of a simple character. It is obvious, however, that an increase in E_n must lead to an increase of the limit energy for knocking off the piece. Therefore, we seek the relation between E_n and $mv^2/2$.

38. An exact answer cannot be obtained from the available equations, but a rough estimate can be made. The axis around which the angular momentum will be taken is the axis 0 at the notch. (Figure 16.) The equations of momentum and angular momentum may be applied for the case of an impact of infinitesimal duration. They are:

$$mv = mv'_x + MV'_x \; ; \qquad (3a)$$

$$mv'_y = -MV'_y \; ; \qquad (3b)$$

$$mvy + iw = mv'_y x + I\omega' + iw' \qquad (4)$$

We assume that

$$E_n = \tfrac{1}{2}\, I\omega'^2 \qquad (5)$$

so that the discussion refers to a shot in which the specimen is barely broken. Also, $V' = Z\omega'$, for an impact at the percussion center. Obviously, there are more unknowns than equations. However, by using Eq. (5) we can rewrite Eq. (4) in a useful form expressing the ratio of E_n and $mv^2/2$. This ratio may be called the energy transfer factor. We find that

$$\frac{E_n}{\frac{1}{2}mv^2} = f = \frac{m}{M}\,\frac{My^2}{I}\,\frac{(1 - v'_x/v)^2}{\left(1 + \frac{i\,(w' - w) - mv'_y x}{I\omega'}\right)^2} \,. \qquad (6)$$

For rectangular bar specimens, My^2/I is about 4/3; and neglecting the terms in parentheses, we obtain the still more approximate value

$$f \cong \frac{4}{3}\,\frac{m}{M} \,. \qquad (5')$$

This indicates that it is desirable to use heavy projectiles so that, with fixed E_n, the bullet energy can be reduced.

39. While the unknowns on the right side of Eq. (6) could all be determined by high-speed photography, and E_n could then be calculated, the test would be so cumbersome that its field of application would be restricted. We must inquire whether the situation can be improved by measurements of other types. Detailed consideration shows that measurement of the force-time curve for the impact would not yield information concerning E_n, but another possibility suggests itself. Work is transmitted downward across any plane in the elastic part of the specimen and if K is the torque across the plane, the magnitude of this work is

$$\int K d\theta .$$

The torque angle curve could be measured by means of resistance gages if the modulus of elasticity of the specimen were known.

40. The work in question goes into plastic energy E_n and elastic wave energy, so it represents an upper limit to E_n. In past investigations we have not attempted to use this method, but have often arranged conditions so that E_n could be estimated from Eq. (6). For example, in our experiments on Mg and Al, using 1/2" spheres, v'/v was always less than .08 and i/I was about .01, while $(w' - w)/\omega'$ was usually less than unity and $mv'_y x/I\omega'$ was negligible. The maximum error incurred by omitting the factors in parentheses is about 20% in this case. In other

cases, these terms may be considerably larger. Sometimes the bullet sticks in the specimen, and then we must put $w' = \omega'$ and $v_x' = V_x' (y/z)$ in Eq. (4). Usually, the bullet rebounds and there is some evidence that with spherical projectiles w' can be placed equal to ω', on the average.

C. Study of Rebound Energy and of Fragments Thrown from the Specimen Face.

41. Our pendulum is a closed structure which catches the projectile and any fragments thrown from the face of the plate, so the pendulum displacement measures the initial value v of the bullet velocity. The energy available to produce plastic flow and ultimate breakage of the specimen depends on the rebound energy of the bullet and the kinetic energy of any fragments which are thrown. We have devised a method for measuring the rebound velocity, and the velocities of typical fragments. We shall illustrate the method by discussing our work on Mg and Al alloys, in which 1/2" spheres were used. Although the impacts were normal, the sphere rebounds at angles which usually lie between 5° and 16°, the average being about 12° in our work on Mg alloys. We attribute the sidewise component of rebound velocity to two effects. The bullet may emerge from our smooth bore gun with considerable spin, and when it gouges out a cavity in the specimen whose depth is more than about three eights of the diameter of the sphere, spin may be developed due to irregularities in friction between the bullet and the cavity. For present purposes, we are not concerned with the magnitude of the sidewise component. To measure the normal component, we bored a hole in a 1/4" plate of 2S aluminum, of Brinell hardness 52 (500 kg. load, 10mm. ball) and placed the plate 8.5" from the specimen (Figure 5) so that the bullet could pass through the hole on its way to the specimen. The rebounding bullet struck the plate in practically all cases, and made a small impression, similar to a Brinell indentation. It was assumed that the size of this indentation was determined by the normal component of velocity. The plate was calibrated by dropping spheres on it from various known heights, from a few inches up to 60 feet, and the relation $v^2 = 2gh$ was used to calculate the velocity and the energy corresponding to each diameter of the indent. Then for each shot, the normal component of rebound velocity or the corresponding energy was found from the curve of velocity vs. indent diameter in Figure 18. It is worth noting that in this speed range the volume excavated (below the original plate surface) is closely proportional to the energy of the sphere.

42. The distribution of the indentations over the surfaces of the rebound-plate is portrayed in Figure 19. The tendency of the impact points to concentrate near a vertical plane near the point of fire is not fully understood, but it may indicate that the bullet makes better contact with the bottom of the gun barrel than with the sides or top. The concentration in a lobe above the plate center may be explained by the fact that the specimen bends back as the bullet penetrates it, or by the overhand spin of the bullet about a horizontal axis. An interesting account of the phenomena encountered in the rebound of golf and baseballs from plates has recently been published by the Bureau of

[redacted]

Standards (Ref. 25); angular velocities of the order of 120 revolutions per sec. were encountered. The conditions in our experiment are quite different but angular velocities of the same order of magnitude are indicated by calculating the ratio of the tangent and normal velocities from the impact points of Figure 19.

43. We find that the energy of rebound in our rupture energy experiments on Mg and Al is in no case greater than 0.3% of the initial energy and that the kinetic energy of rotation of the projectile is negligible in Eq. (2). These remarks do not apply to the corresponding momentum terms in Eqs. (3) and (4). Some alloys lost fragments at the front surface in the vicinity of the sphere. In many cases these fragments hit the 2S aluminum plate at the front of the pendulum, leaving an impression. A typical group of fragments was collected from several shots with the result that 29 pieces weighed a total of 60 grains. This would give an average of 2.1 grains. Undoubtedly smaller fragments came off, which could not be found, and this would lower the average weight of a fragment.

44. Four of the largest fragment indents were selected and measured to find their volume. The energy necessary to make these indents was approximated by comparison with the results of the sphere dropping experiment. For the spheres, a curve of volume displaced vs. kinetic energy was plotted. Then using the volume of the fragment indents the kinetic energy was read from the curve. The average energy of these 4 fragments was found to be 0.30 ft. lbs. This energy corresponds to dropping a sphere from a height of 15 ft. Since the fragments weigh only 1.5% as much as the sphere, they must be traveling about 8 times faster or 260 ft/sec. on the average. A study of the plate-front spalling on all available magnesium specimens indicates that the bullet energy need not be corrected for the total energy of the fragments, which appears to be one per cent of the bullet energy or less.

DECLASSIFIED

CONCLUSIONS V

45. Sufficient work has been done to demonstrate the utility of the ballistic bend test. It is simple, rapid and accurate and there seems to be no reason why customary impact tests at striker speeds of 10 to 20 feet per second should be employed in studies of shock damage occurring at very high strain speeds. Currently, experiments are under way on the energy required for crack propagation in certain metals, by applying the ballistic bend test to precracked specimens. We may anticipate that eventually experiments of this kind will play a large part in designing materials to withstand high-speed damage.

[redacted]

DECLASSIFIED

APPENDIX I

SURVEY OF WORK ON THE DYNAMICS OF PLASTIC FLOW

(The following discussion applies to the facts presented in Section IB.)

1. Plastic Waves. In this section we shall review a simple case of plastic wave propagation, that in which the end of a semi-infinite uniform bar is given a longitudinal impact. The loading device imparts a velocity v to the end of the bar. The velocity of a longitudinal elastic wave along an infinite bar is $(E/\rho)^{1/2}$ where E is Young's modulus and ρ is the density; but Young's modulus is the slope of the stress-strain curve in the elastic region, so the wave velocity is proportional to the square root of the slope. Similarly, the small plastic deformation which produces a particular increment of strain at a chosen point will pass that point with a velocity which is proportional to the slope of the tensile stress-strain curve. This slope is, of course, the one appropriate to the instantaneous plastic strain e existing at the point. For reasons explained in the literature, the curve showing apparent stress, or load over original area, as a function of strain, should be employed. For most metals this slope decreases steadily as the strain increases, and when this is the case the successive strain-increments travel with velocities which get smaller as the deformation increases. Eventually, the slope of the tensile stress-strain curve must become zero, and this corresponds to the condition of instability which leads to cracking and to fracture. (In compression tests the slope may increase over a certain strain region, and this case has been separately considered by White and Griffis. In bend tests, the situation is complicated by the inhomogeneous deformation, which leads to a variation of the wave velocity as we pass from the specimen surface toward the neutral axis.)

2. It is qualitatively clear that when a bar is given a sufficient tensile impact load at one end, A, it should fail, theoretically, at that end, and practically, near that end. Consider a piece, AB, having mass M. If the force on the end is F, and the acceleration is a, the stress at point B would be F-ma, if stress were propagated with infinite velocity. This picture of stress-decrease along the bar must be modified as follows to take the finite speed of the deformation-pulse into account.

(a) Elastic Case. Let one end of the bar, at $x = 0$, be set into motion at zero time with a constant velocity v, and let the speed of the elastic wave-front be

$$c_o = \sqrt{E/\rho}$$

The wave equation, under the assumed conditions, yields the following values of stress and strain:

$$S = \rho v c_o \; ; \; e = v/c_o, \qquad (1)$$

[redacted]

which apply at all points up to the position $x = c_0 t$. This solution does not indicate any decrease of stress or strain as x increases, because the usual elastic wave equation assumes that the displacements are infinitesimal and that the wave velocity is constant.

(b) Plastic Case. Important changes are encountered when we deal with larger strains, for two reasons. As mentioned above, the greater the strain, the smaller the velocity of an increment of strain. Also the change of cross-section and the finite velocity of each element of the medium must be taken into account. The net result is that strain varies as we pass from $x = 0$ to $x = c_0 t$, in the following way. Near the origin, from $x = 0$ to $x = v't$, the strain comes up to a value which satisfies the relation

$$v' = \int_0^e \left(\frac{dS/de}{\rho} \right)^{\frac{1}{2}} de; \qquad (2)$$

as von Karman showed (Ref. 1). This relation replaces the elastic-theory relation, $v = c_0 e$. We can get a physical understanding of von Karman's results by observing that all elements in this range have come up to a velocity sufficient to prevent further acquisition of strain-energy from the loading device. Namely, the velocity v' given by Eq. (2), and this velocity agrees with the speed of the striker. The work-hardened portions of the bar between $x = 0$ and $x = v't$ merely act as a piston or plunger, to transmit the stress to other elements beyond. The latter elements respond until they also reach the full strain corresponding to velocity v'. Thus the "fully strained" region continually encroaches on the "intermediate region". In the intermediate region, from $v't$ to $c_0 t$, the strain drops off from the value given by (2) to the value v/c_0 given by (1).

3. Its approximate value, at any x and t, is obtained from

$$(dS/de)/\rho = x^2/t^2 \qquad (3)$$

Using this to evaluate dS/de, we can then employ a plot of dS/de against e to determine the value of e at position x and time t.

4. Now we can see clearly that when e reaches the value corresponding to the tensile strength, the bar must neck, close to the loaded end, at some point determined by local weakness. This will happen at a definite value of the impact velocity which is called the critical speed in tension. The values determined by carrying the integration in Eq. (2) up to the elongation corresponding to the tensile strength are often in fairly good agreement with experimental results. (Ref. 3). The critical speeds found are usually from 100 to 200 feet per second. It should be understood that the critical velocity depends on the type of loading, since the stress strain curves for various types are different. For example, the following figures for annealed copper have been given:

[redacted]

Loading	Critical Velocity, fps.
Tensile	160
Transverse (wire)	450
Compressive	600

Arising as they do from inertial causes and from work hardening, these speeds should not be confused with critical strain rates at which the type of fracture changes. In some cases, the experimental and theoretical values do not check and it appears possible that the results are influenced by a change in fracture type. This is made plausible by the fact that such changes may occur in Izod or Charpy impact testing of steels whose transition temperatures lie in the neighborhood of room temperature.

5. Tensile Impact Tests. The chief point to be considered here is the velocity dependence of (1) strength quantities, (2) elongation and reduction, and (3) work absorbed up to the point of rupture. In the speed range covered by "static" testing machines there may be complicated effects (Ref. 4) due to strain-aging or to relaxation during the test. For the most part, we shall overlook these complications, confining our attention to the more prominent effects which are encountered when we compare the static behavior with the results obtained at the speed of an Izod or Charpy test, and at still higher speeds. Most of the results quoted are obtained from the work of Manjoine and Nadai (Ref. 4) and the extensive experiments of Duwez, Clark, Wood, and their collaborators at California Institute of Technology (Refs. 2,3.). In the latter experiments the impact velocity runs up to about 200 fps. Customarily, specimens without notches are used and it must be understood that strain rates do not exceed a value of several hundred inches per inch per second. The highest strain rates we have encountered in tensile impact tests were achieved in work done at Massachusetts Institute of Technology by de Forest and his colleagues, reported by Roop and Carrigan (Ref. 5). In these tests the specimen was located in the central cavity of a device composed essentially of two concentric cylinders. An explosive charge arranged in the form of a ring was used to drive the two halves of the cylinder apart, rupturing the specimen. The oscillograph records for specimens of medium steel indicate strain rates running up as high as 16000 per sec., although the average is much lower. These values are comparable with those encountered in the plastic flow of armor in penetration tests.

6. In the ductile metals commonly studied, the stress at a given strain usually increases with velocity. This is in accordance with a well known theory proposed by Becker. Of course the tensile strength may decrease when a material very sensitive to velocity, such as pitch, changes its mode of fracture from the ductile to the brittle form. We shall neglect such instances, which are not of much interest to the student of metals.

7. In general, metals show an increase of tensile strength in the range of impact velocity from zero to 25 feet per second and very little change over the range 25 to 200 feet per second. The increase runs from zero to about 50%.

[redacted]

8. The work by Duwez, Clark, Wood and their associates has revealed three principal types of behavior of the elongation.

(a) The elongation changes a few per cent in going from static tests to about 25 fps, then remains constant up to the critical velocity. The low-speed change may be an increase or a decrease. Examples are as follows:

SAE 1020, annealed	Increase
Armco iron, annealed	Decrease
Spheroidized high carbon steel	"

(b) The elongation increases regularly up to a maximum and then decreases regularly. An example is SAE 1020, cold rolled. The authors state that this type of behavior has been found only in cold rolled material.

(c) The elongation increases slightly and finally decreases with considerable scatter at all velocities employed. An example is SAE 2345, quenched and tempered to a hardness of 52 Rockwell C.

9. We are inclined to believe that this classification is somewhat artificial and that all intergrades of behavior will eventually be found. Duwez and Clark do not mention the extensive slow bend and impact tests of Petrenko (Ref. 15), who studied a number of ferrous and non-ferrous materials. These tests were carefully done and they reveal a certain general pattern of behavior. All non-ferrous metals tested by Petrenko showed an impact work higher than the static work. As to steels, increase of speed usually leads to an increase of work, with the exception that microstructures of high hardness and of low elongation show a decrease.

10. <u>Compression Impact Tests.</u> Tests of copper in compression (Ref. 8) at strain rates up to 1600 per sec. show that the dynamic stress is already about 25% higher than the static stress at a rate of 30 per sec. and there is no appreciable increase thereafter. This checks the usual behavior encountered in the tensile impact test.

11. <u>Bending Impact Tests.</u> The work of Petrenko was mentioned above. Another important series of tests between "static" speed and Izod speed was made by Docherty, using both ferrous and non-ferrous materials. Just a few noteworthy points will be reported here:

(a) Decrease of work with increase of speed were reported for a medium carbon steel and for a 3% nickel steel both in the normalized condition. These materials would not be expected to show a change of fracture type in these room temperature tests, and the matter requires further investigation, because, if the results can be confirmed on similar material, we have here an exceptional type of behavior.

(b) Annealed monel, in the range of impact speeds from 7×10^{-5} fps to 8×10^{-3} fps, showed an increase of rupture work much larger than

[redacted]

that of any material so far investigated. This increase, amounting to about 20% for a tenfold change of speed, may be compared with a corresponding effect of 3 to 7% in the case of many other metals. The behavior of monel in the as-rolled condition is in no way out of the ordinary. These results agree precisely with the findings of Petrenko, working on monel several years earlier. In fact the numerical agreement is so close that it must be fortuitous.

12. Criticism of Conventional Impact Tests. As stated earlier, notch-bend tests carried out on conventional impact machines yield strain rates before cracking which are sometimes higher and sometimes lower than those attained in recent tensile impact tests with unnotched bars. The notch-bend strain rates may lie below or above the critical strain rate, calculated for the case of tension. (See Section I-B) The customary striking velocities in commercial machines run from 11.4 to 18.1 fps, but in some machines the height of pendulum fall is adjustable over a large range. Rough values of the strain rates, calculated on the conventional basis indicated in Section IV-A of this report, are presented in the schedule below:

Notch	Striker Speed, fps. 10	20
Charpy keyhole, 2mm diameter,		
Struck at middle:	175	350
Struck 22mm. from middle	350	700
Izod notch, 0.5mm. diameter,		
Struck at middle:	700	1400
Struck 22mm. from middle	1400	2800

These are initial strain rates and it is clear that if the specimen absorbs a large fraction of the energy, the strain rates may be much smaller during the later part of the fracture process. Strain rates near the crack head will of course be very large, but much plastic flow occurs at the notch before cracking, and also in regions well ahead of the advancing crack. This flow may be accomplished at strain rates less than the critical one. It is clear from the table that this situation would be favored by the use of a Charpy specimen with low striking velocity. On the other hand, the use of a double-width specimen would increase the constraint at the center of the notch, which would probably reduce the critical velocity. Referring to formula (2), increase of constraint should raise the values of the integrand but should reduce the upper limit of the integral, and we anticipate that usually the net effect will be a decrease of v'.

13. All these remarks indicate at least one cause for instability of impact energies. It may occur that one specimen has a critical strain rate just above the actual strain rate at the commencement of the test, so that considerable energy is absorbed in the early stages, and the strain rate in the regions undergoing plastic flow remains below the critical point through-out the test. Another specimen, having a slightly lower critical velocity, may permit the maintenance of higher strain

[redacted]

rates throughout the test and thus cause a low impact value. Similar remarks apply if the strain rate is chosen to correspond to the borderline between ductile and brittle fracture. Further, it may happen that exceeding the critical velocity for the specimen as a whole results in a restriction of the flow region and an increase of strain rate sufficient to induce the transition from ductile to brittle fracture. In such a case the two effects would not be distinguished.

14. At this point investigators of impact phenomena will probably be inclined to object, on the basis that curves of impact work versus temperature usually exhibit a single drop, associated with suppression of the slip mechanism, which leads automatically to higher strain rates at lower temperatures. The double mechanism postulated above requires that in general there should be a drop associated with the act of exceeding the critical velocity, and another associated with the change from ductile to brittle fracture. To this we reply that critical-velocity phenomena have been clearly revealed by the California Institute investigations and that they may help greatly in clearing up puzzling features of earlier investigations such as those of Mann and his colleagues (Ref. 6); that critical-velocity phenomena have not yet been sufficiently studied for cases of inhomogenous deformation; that the shapes of temperature-transition curves vary greatly and there are many cases where the impact value changes considerably outside the temperature-range arbitrarily picked out as the transition region; also that there is plenty of room for impact studies in which both the temperature and the speed are varied. In view of the figures in the above table it is quite reasonable to suppose that critical-velocity phenomena do not play any important part in tests with the relatively sharp Izod notch, but the possibility that they do play a part should be kept in mind until the matter is settled by experiment.

[redacted]

REFERENCES

Reference (1) T. von Karman, On the Propagation of Plastic Deformation in Solids, OSRD Report 365.

Reference (2) P. E. Duwez and D. S. Clark, Influence of Impact Velocity on the Tensile Properties of Some Metals and Alloys, OSRD Report 3837. (A survey of the effects of speed on 24 ferrous and 12 non-ferrous alloys.)

Reference (3) Clark, Hyers, Wood, and Duwez, Mechanics of the Dynamic Performance of Metals, OSRD Report No. 4343.

Reference (4) M. Manjoine and A. Nadai, High Speed Tension Tests at Elevated Temperatures; Part 1, Proc. ASTM, 40, 822, 1940; Parts II and III; J. Applied Mechanics, June 1941; Trans. ASME, page A 77, 1941. Manjoine, Influence of Rate of Strain and Temperature on Yield Stresses of Mild Steel, J. Applied Mechanics, 11, p. A-211, 1944.

Reference (5) W. P. Roop and H. I. Carrigan, Properties of Medium Steel at High Rates of Loading, Report No. 503 of the David W. Taylor Model Basin.

Reference (6) R. C. Haskell and H. C. Mann, General Discussion of the Notched Bar Test, Trans. Manchester Assoc. of Engineers, p. 119, 1937-8.

Reference (7) P. G. Jones and H. F. Moore, Effect of Strain Rate on the Results of Tension Tests, A.S.T.M. 40, 610 (1940).

Reference (8) F. Seitz, The Testing of Metals in Compression at High Rates of Strain. OSRD Report No. 1388.

Reference (9) Ruark, Shearin, Trimble, Rosen and Cooper, Studies of Size Effect in Heavy Class B Armor Steel, Progress Report No. 20 from Department of Physics, University of North Carolina to Naval Research Laboratory.

Reference (10) Ruark, Shearin, Trimble and Michie, Size Effect in Armor Steels and Other Metals, Naval Research Laboratory Report No. 0-2412.

Reference (11) J. H. Hollomon, The Notched Bar Impact Test, Metals Technology, Paper 1667, April 1944.

Reference (12) J. G. Docherty, Effect of Velocity of Test on Notch Brittleness, Engineering 126, 597 (1928).

Reference (13) E. R. Parker and E. A. Smith, High-Speed Tensile Impact Tests on Single Crystal and Polycrystalline Bars of Copper. Metals Technology, Paper 1704, April 1944.

[redacted]

REFERENCES (Cont'd)

Reference (14) M. P. White and Le Van Griffis, Wave Propagation in a Uniform Bar whose Stress-Strain Curve is Concave Upward. N.D.R.C. Report No. A-152.

Reference (15) Petrenko, Technical Papers of the Bureau of Standards, 19, 315 (1925).

Reference (16) NRL Report No. O-2532. Bend Testing at Ballistic Speeds. Second Partial Report. Tests of Magnesium Alloys and of 24ST Aluminum. H. L. Smith and Arthur E. Ruark, 15 May 1945.

Reference (17) H. W. Gillett, Impact Resistance and Tensile Properties of Metals at Subatmospheric Temperatures; separate publication of A.S.T.M., 1941, Philadelphia, Pennsylvania.

Reference (18) Jackson, Donaldson, Laxar, and McKenna, NRL Report No. M-2050, Shock Fracture Test for Welded Joints in Armor, 26 April 1943.

Reference (19) Donaldson, Laxar, McKenna, and Jackson, NRL Report M-2163, Second Partial Report on NRL Shock-Fracture Test for Welded Joints, 4 Sept., 1943.

Reference (20) McKenna, Laxar, and Jackson, NRL Report M-2306, Third Partial Report on NRL Shock Fracture Test for Welded Joints, May, 1944.

Reference (21) McKenna and Laxar, NRL Report M-2453, Fourth Partial Report on NRL Shock-Fracture Test for Welded Joints in Connection with Qualification of Unionmelt Welding of STS Armor, 30 January 1945.

Reference (22) Kramer, Tolman, and Haswell, NRL Report No. M-2328, The Thermal Behavior and Mechanical Properties of Iron-Manganese and Iron-Manganese-Nickel Alloys, July 1944.

Reference (23) Kramer, Tolman, and Haswell, NRL Report No. M-2393, High-Manganese-Nickel Alloys for Heavy Armor and Forgings, November 1944.

Reference (24) Irwin, NRL Report No. O-1778, Ninth Partial Report on Light Armor, 4 Sept., 1941.

Reference (25) Briggs, L. J., Methods for Measuring the Coefficient of Restitution and the Spin of a Ball, J. Research Bur. Standards, 34, Jan. 1945.

Reference (26) Kramer, Haswell and Smith, High-Velocity Shock Tests on Steel from an 18-inch Armor Plate, NRL Report No. June, 1945.

[redacted]

FIG. 1

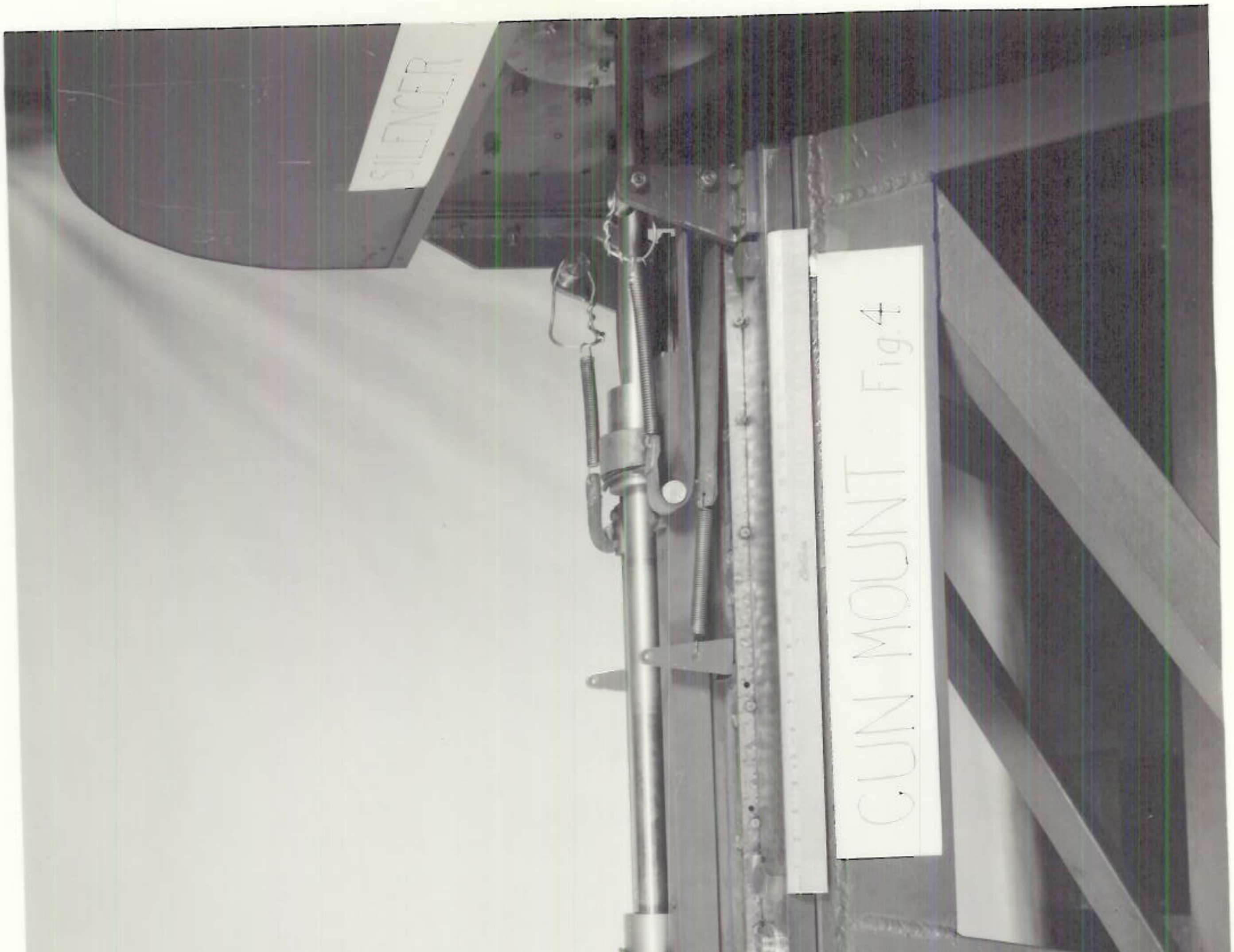

DECLASSIFIED

FIG. 2

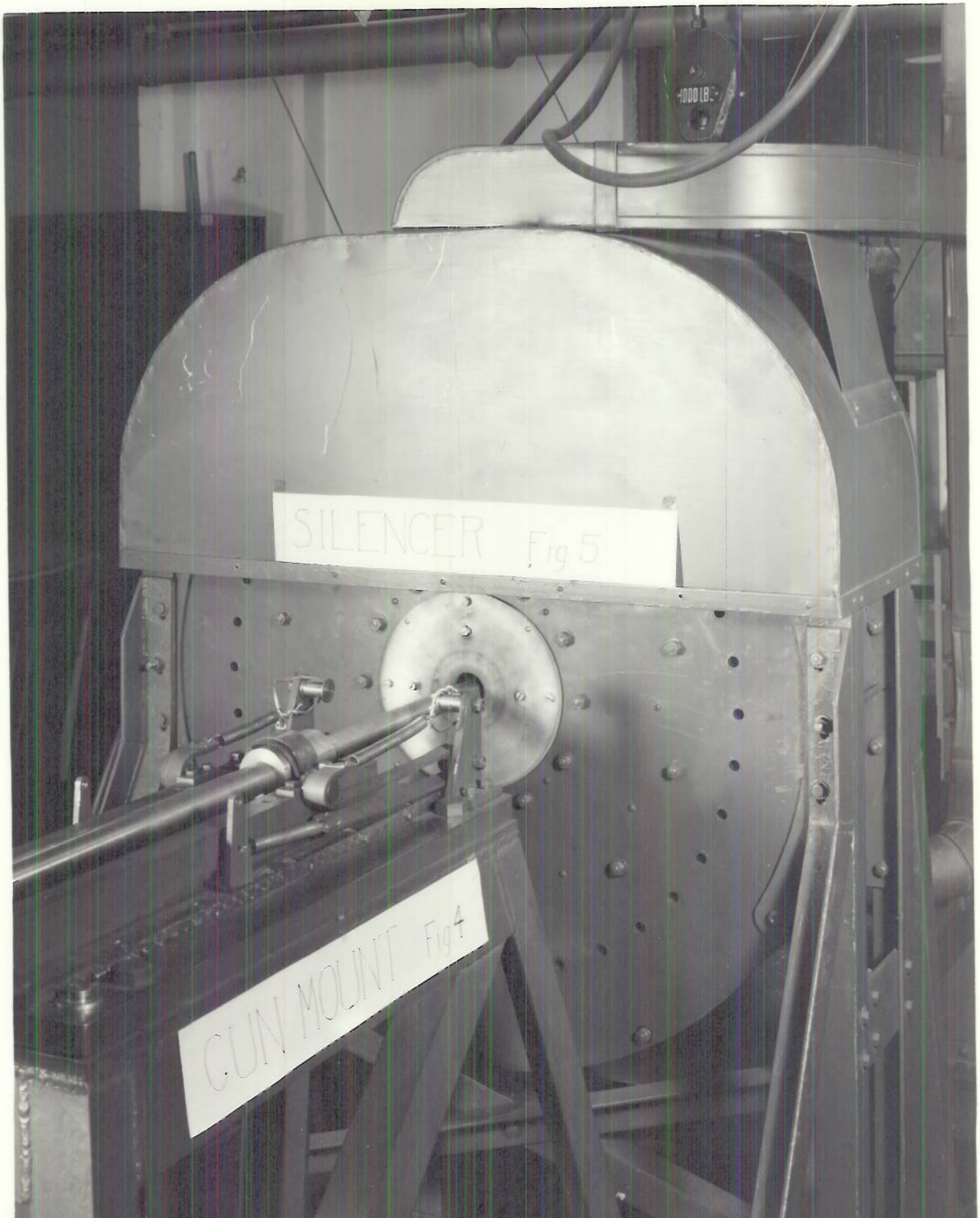

DECLASSIFIED

FIG. 3

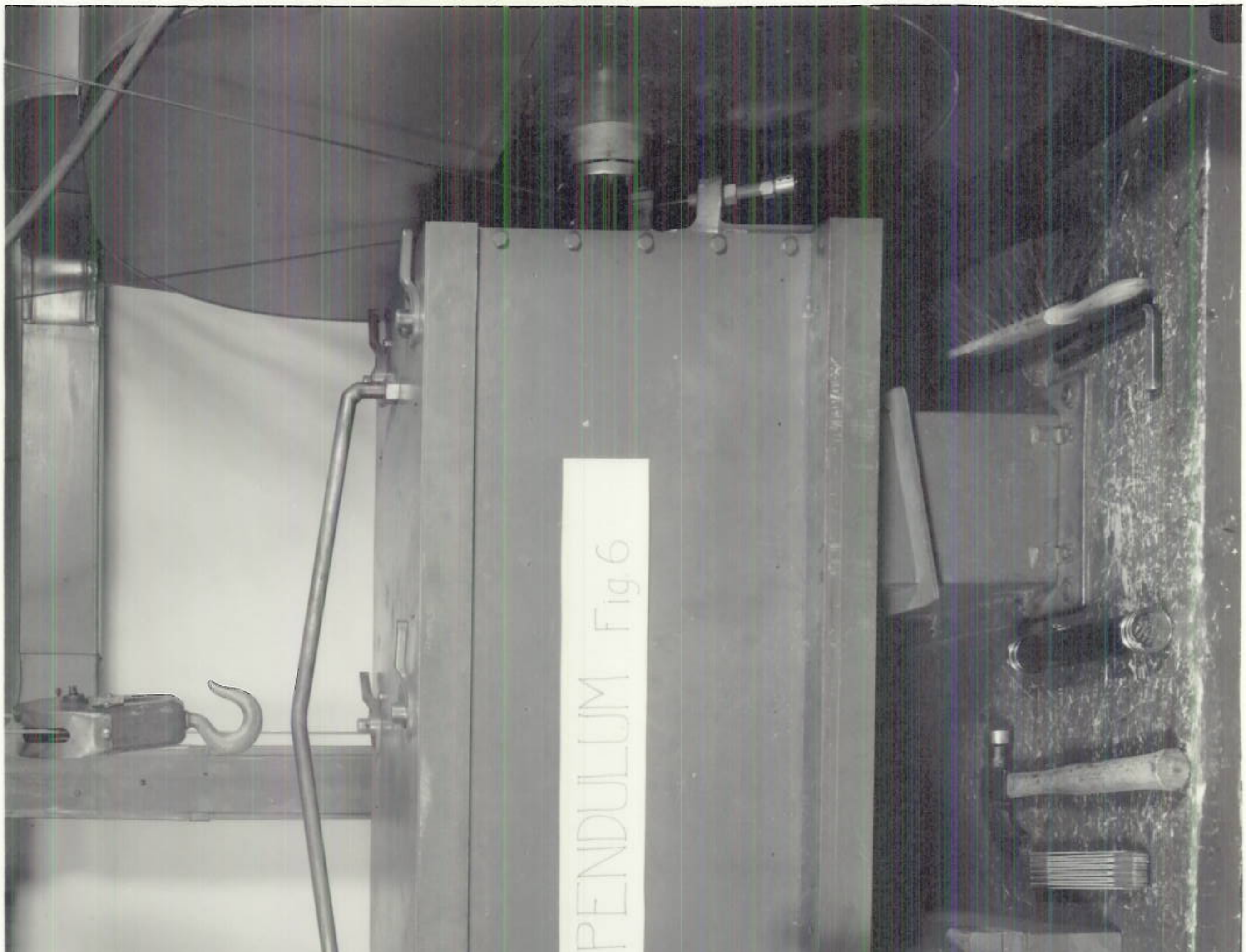

FIG. 4

FIG. 5

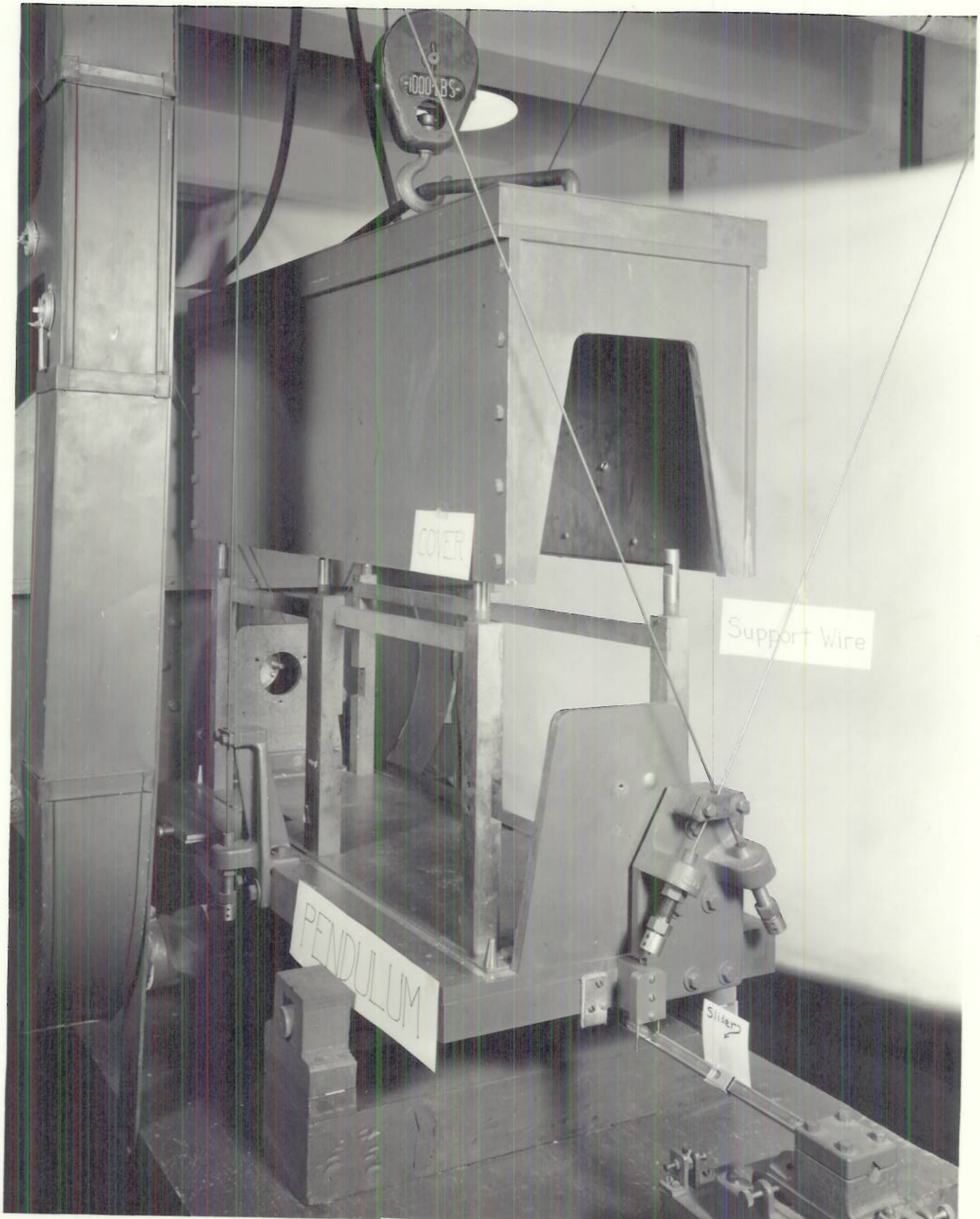

DECLASSIFIED

FIG. 6

FIG. 7

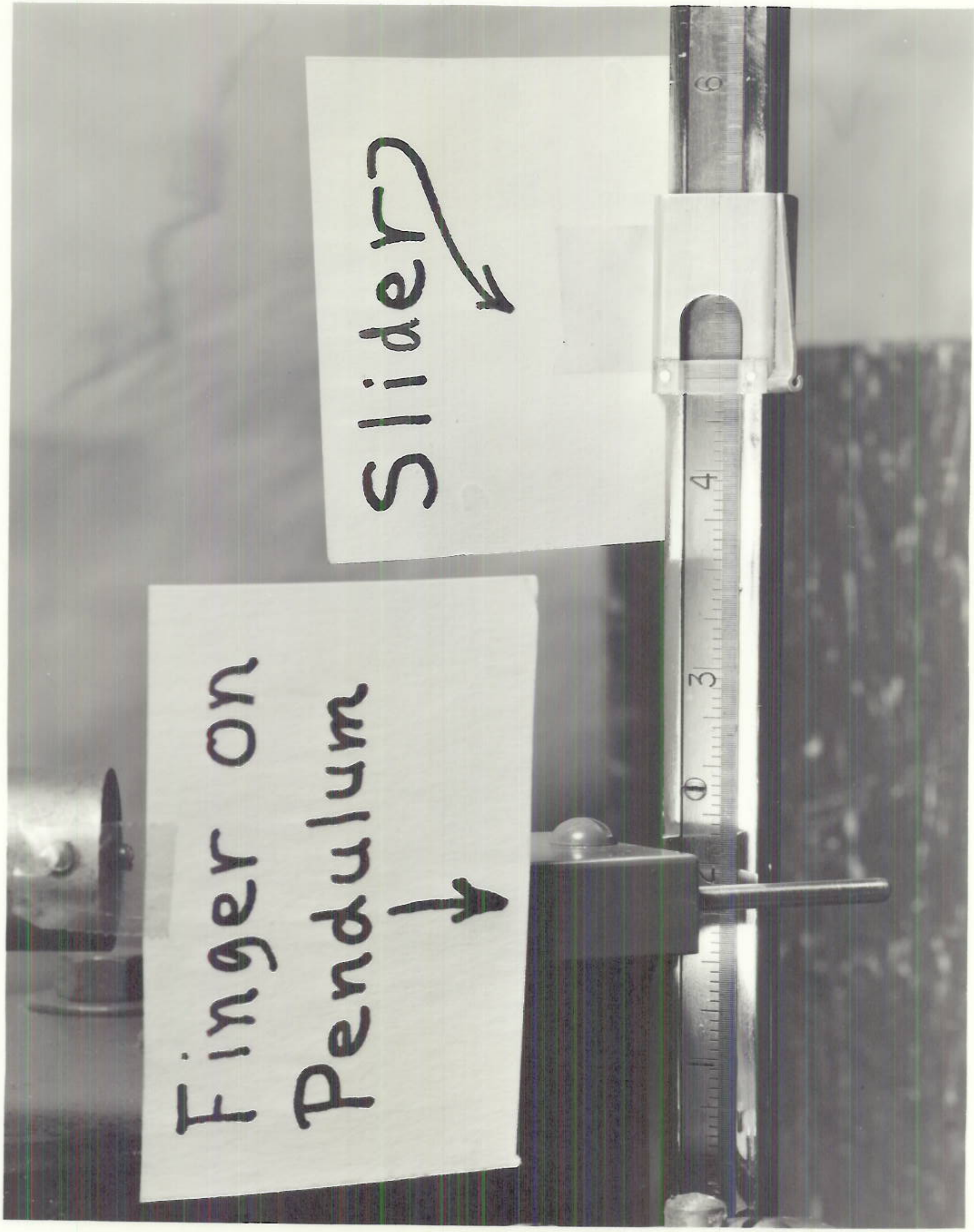

DECLASSIFIED

FIG. 8

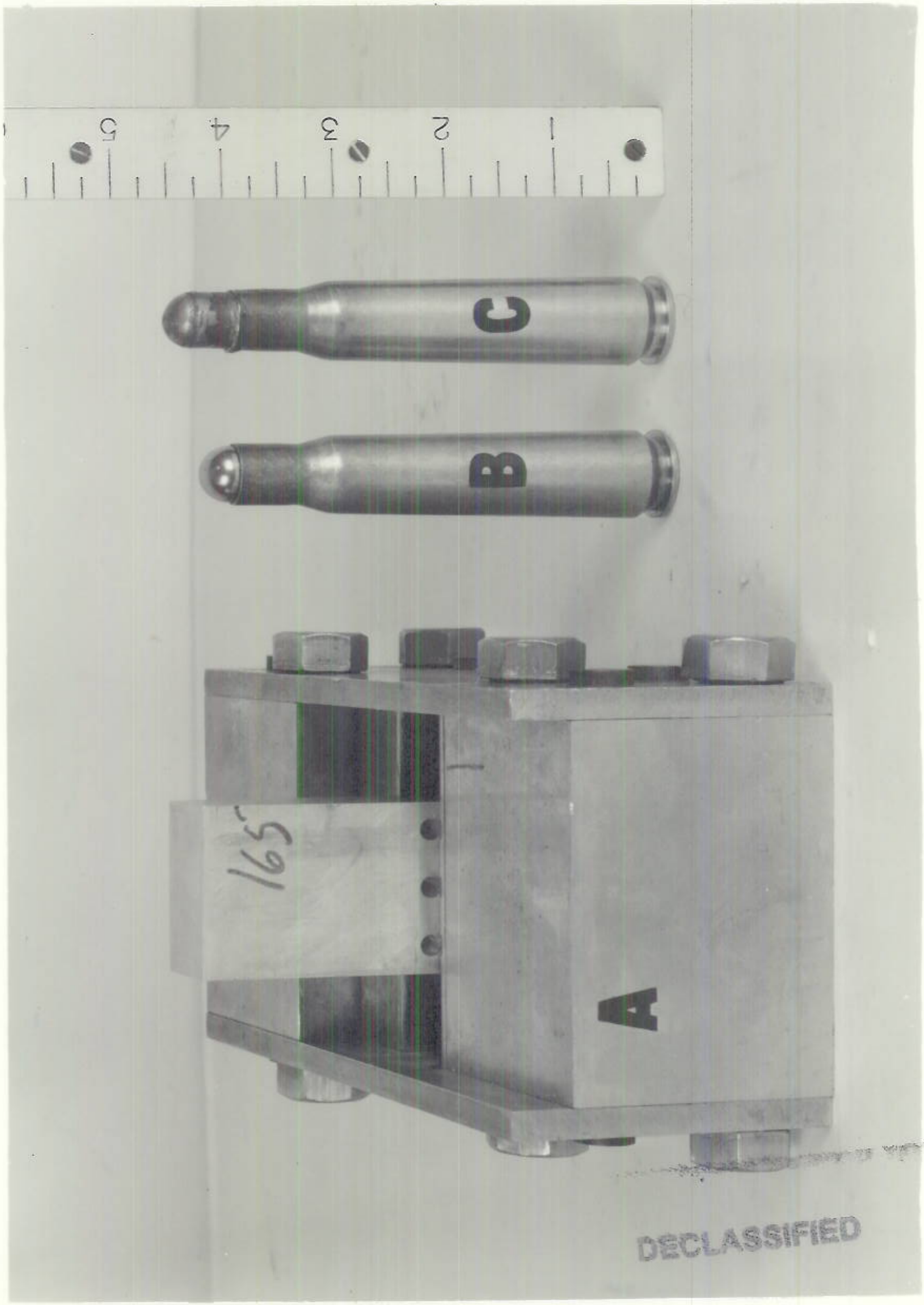

DETAIL VIEW OF JIG, SPECIMEN & PROJECTILES
A - JIG
B - 128 GRAIN SPHERE PROJECTILE, 50 CAL. CASE
C - 240 GRAIN PROJECTILE, 50 CAL. CASE

FIG. 9

100 POUND JIG USED FOR HOLDING NRL SHOCK FRACTURE SPECIMENS

FIG. 10

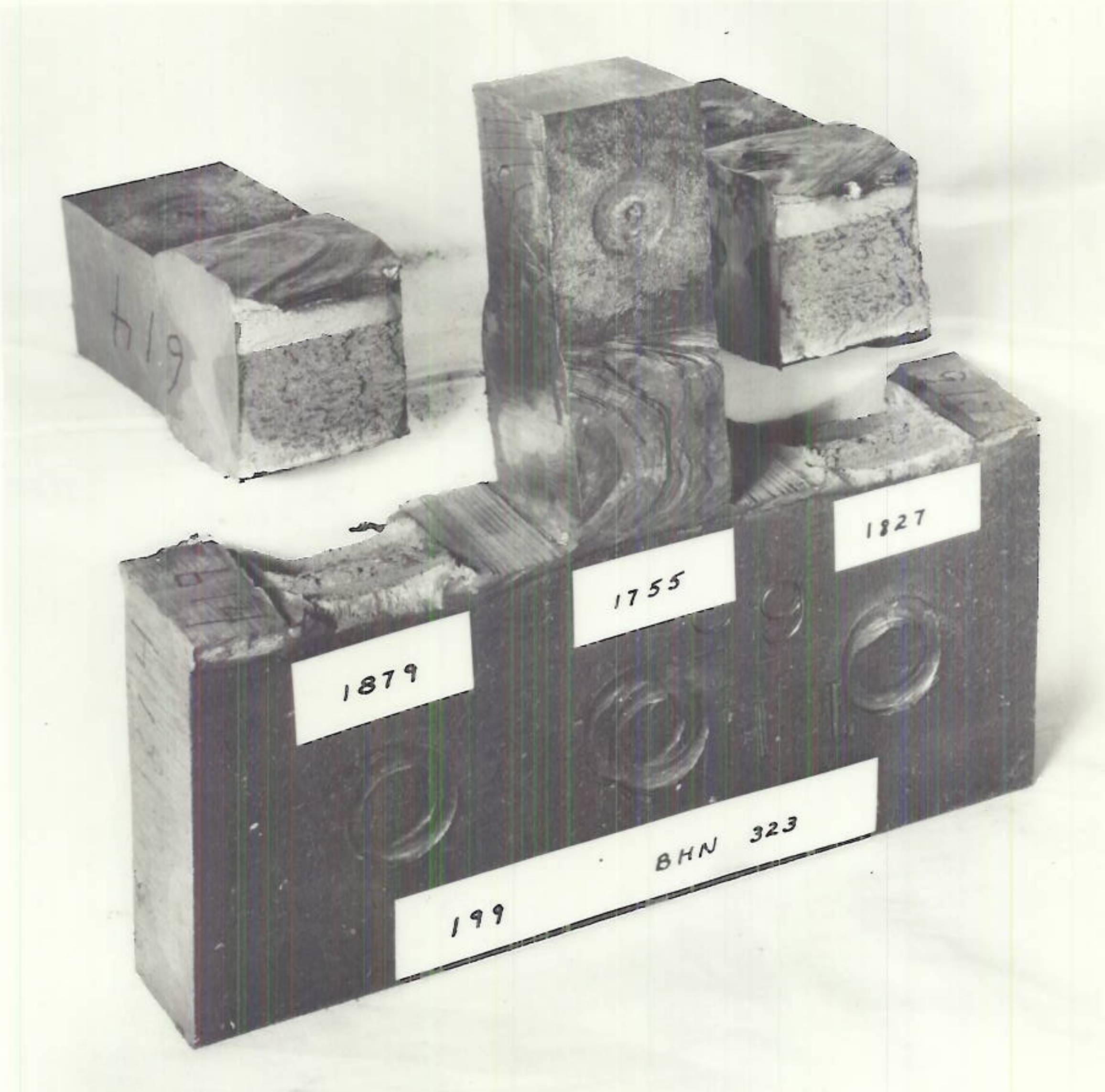

NRL SHOCK FRACTURE SPECIMEN. DOUBLE V WELDS AT BASE OF FINGERS.

FIG. 11

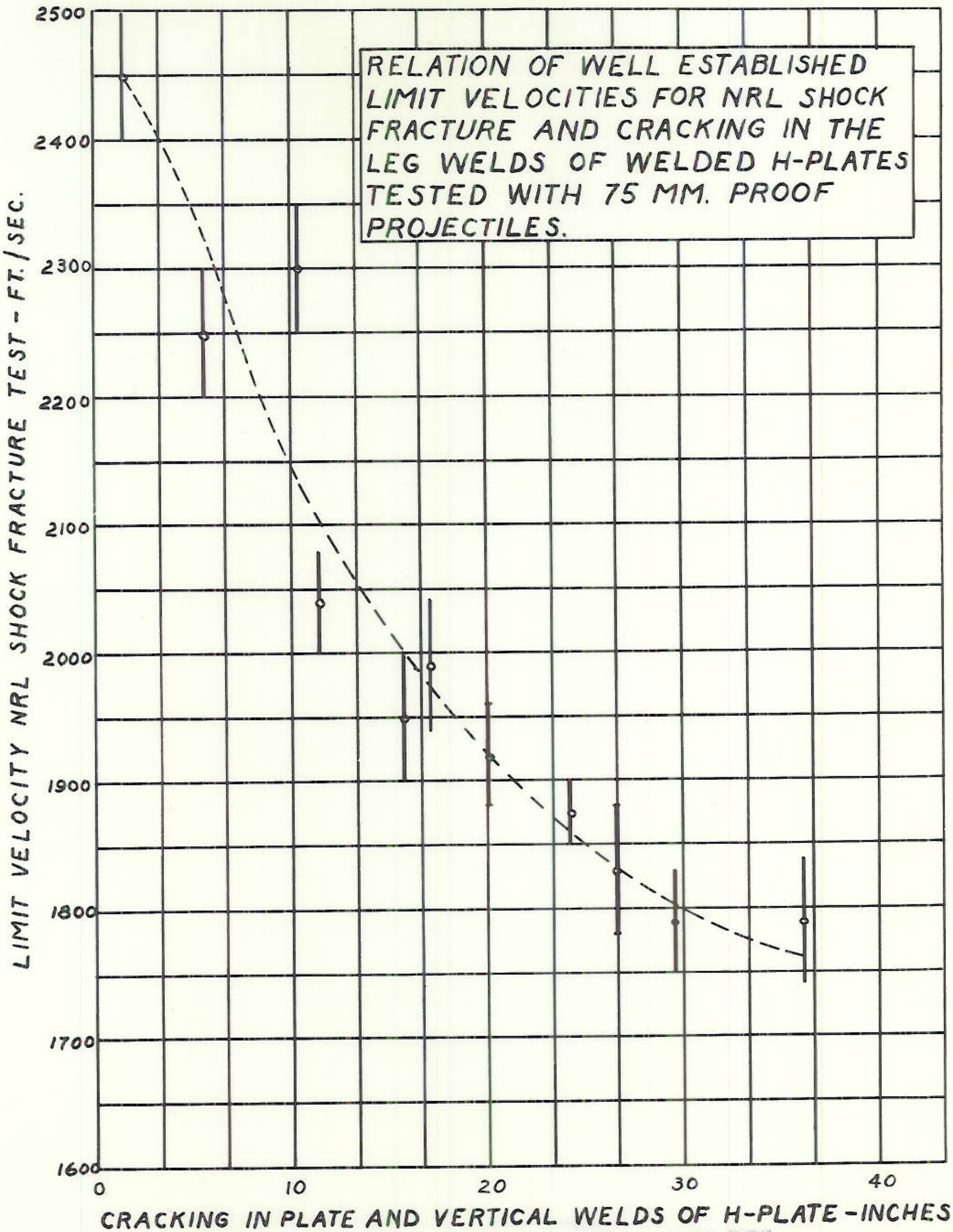
RELATION OF WELL ESTABLISHED LIMIT VELOCITIES FOR NRL SHOCK FRACTURE AND CRACKING IN THE LEG WELDS OF WELDED H-PLATES TESTED WITH 75 MM. PROOF PROJECTILES.
LIMIT VELOCITY NRL SHOCK FRACTURE TEST - FT./SEC.
2500
2400
2300
2200
2100
2000
1900
1800
1700
1600
0
10
20
30
40
CRACKING IN PLATE AND VERTICAL WELDS OF H-PLATE-INCHES

FIG. 12

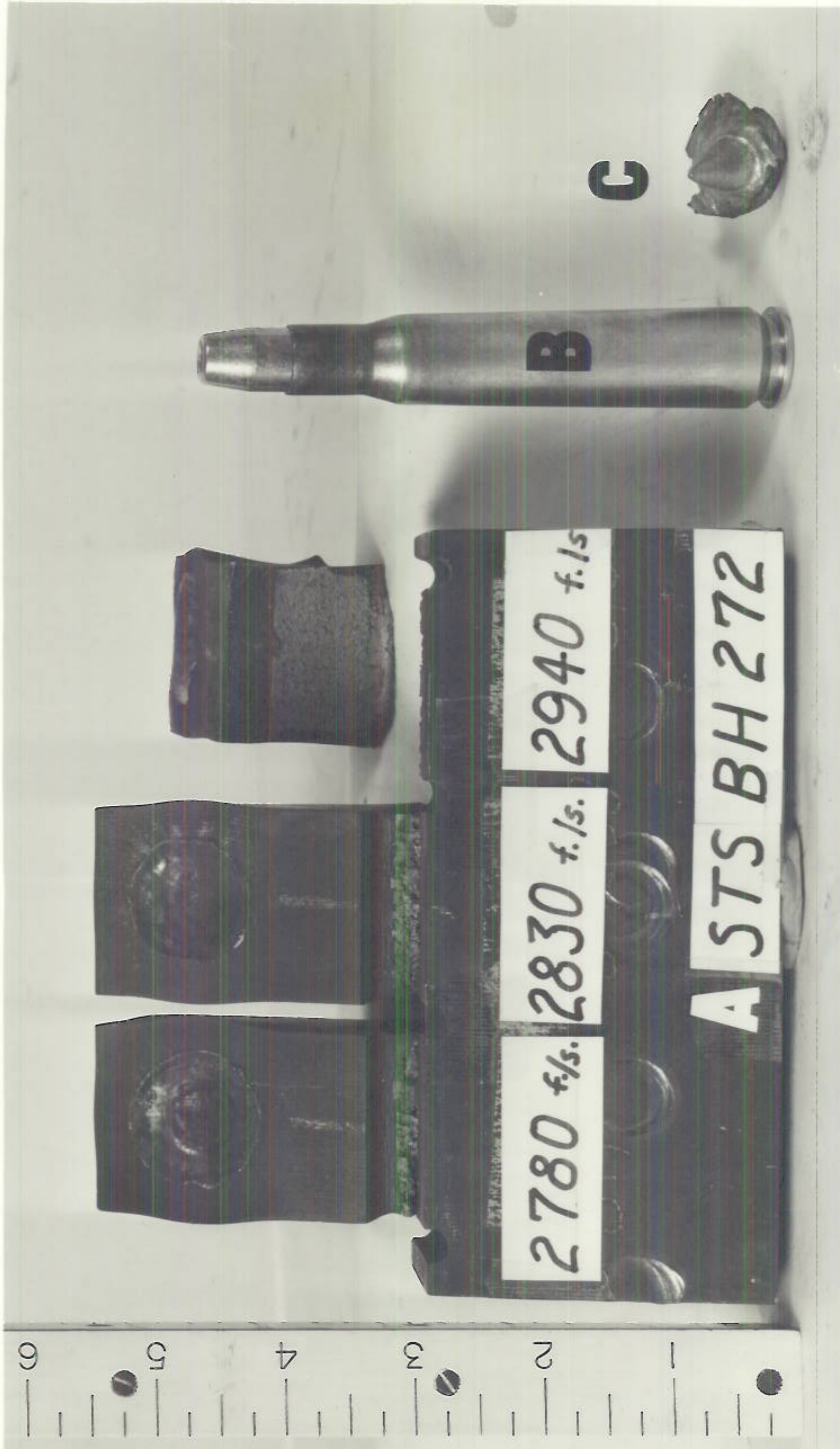

A SHOCK FRACTURE NOTCHED STEEL SPECIMEN.

B M2 BALL AMMUNITION 700 GRAINS SHOT BACKWARD.

C DEFORMED BULLET AFTER SHOT.

FIG. 13

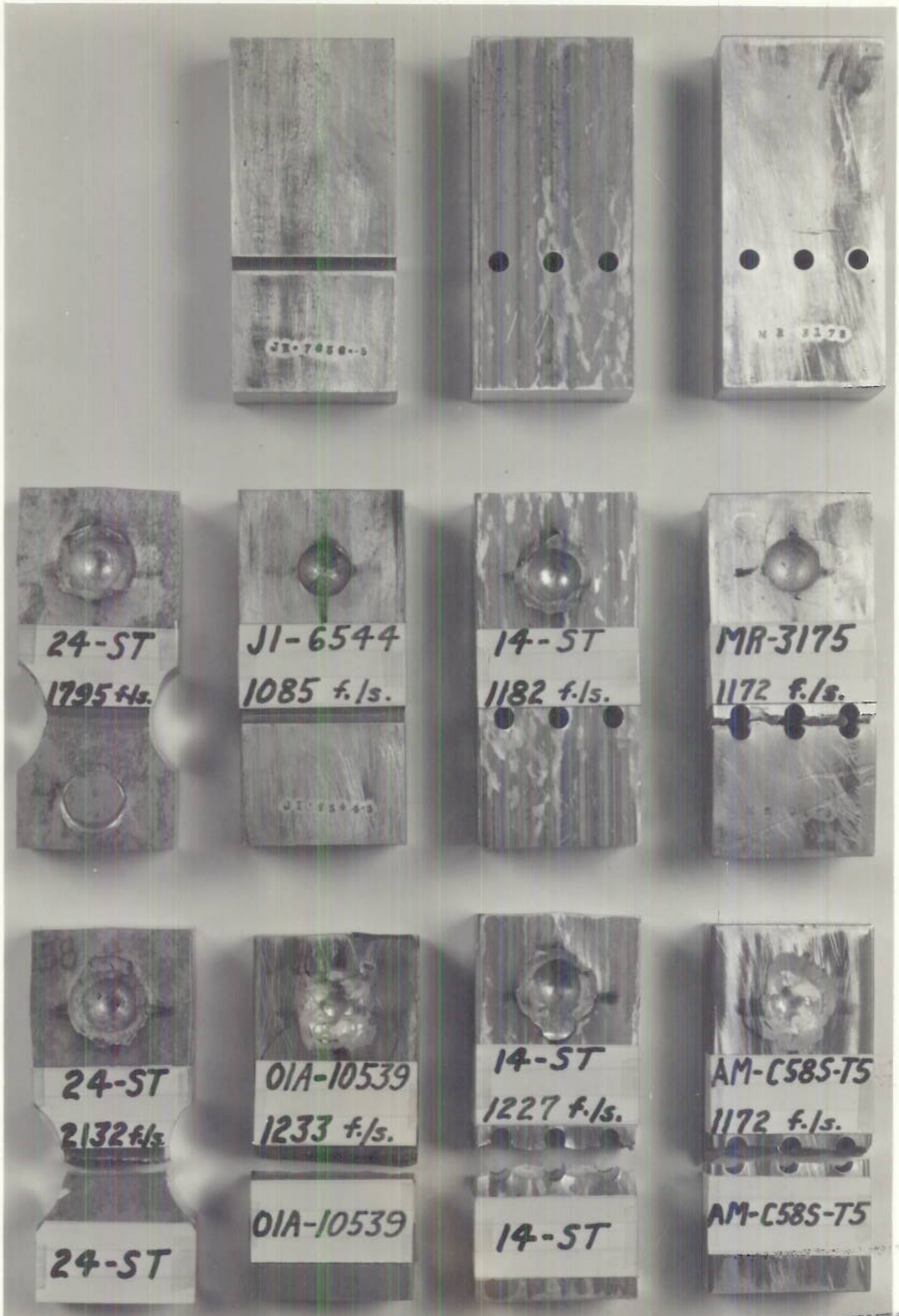

BALLISTIC BEND SPECIMENS;
ALUMINUM & MAGNESIUM ALLOYS.
DRILLED TYPE IS UTILIZED IN COMPARING
ROLLED BARS AND EXTRUDED BARS.

FIG. 14

FRACTURE OF ALUMINUM & MAGNESIUM NOTCH & DRILL SPECIMENS

FIG. 15

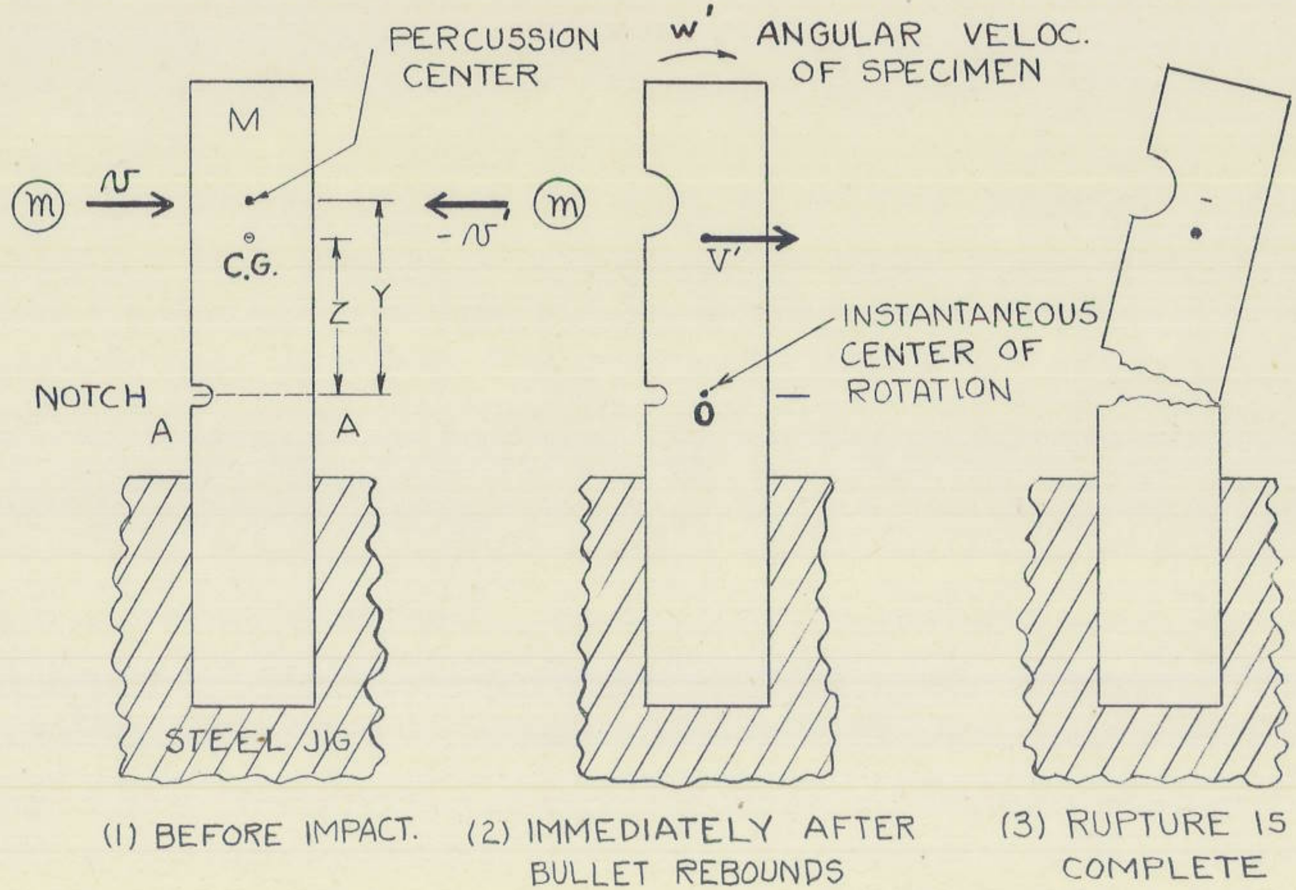

FIG. 16.

DECLASSIFIED

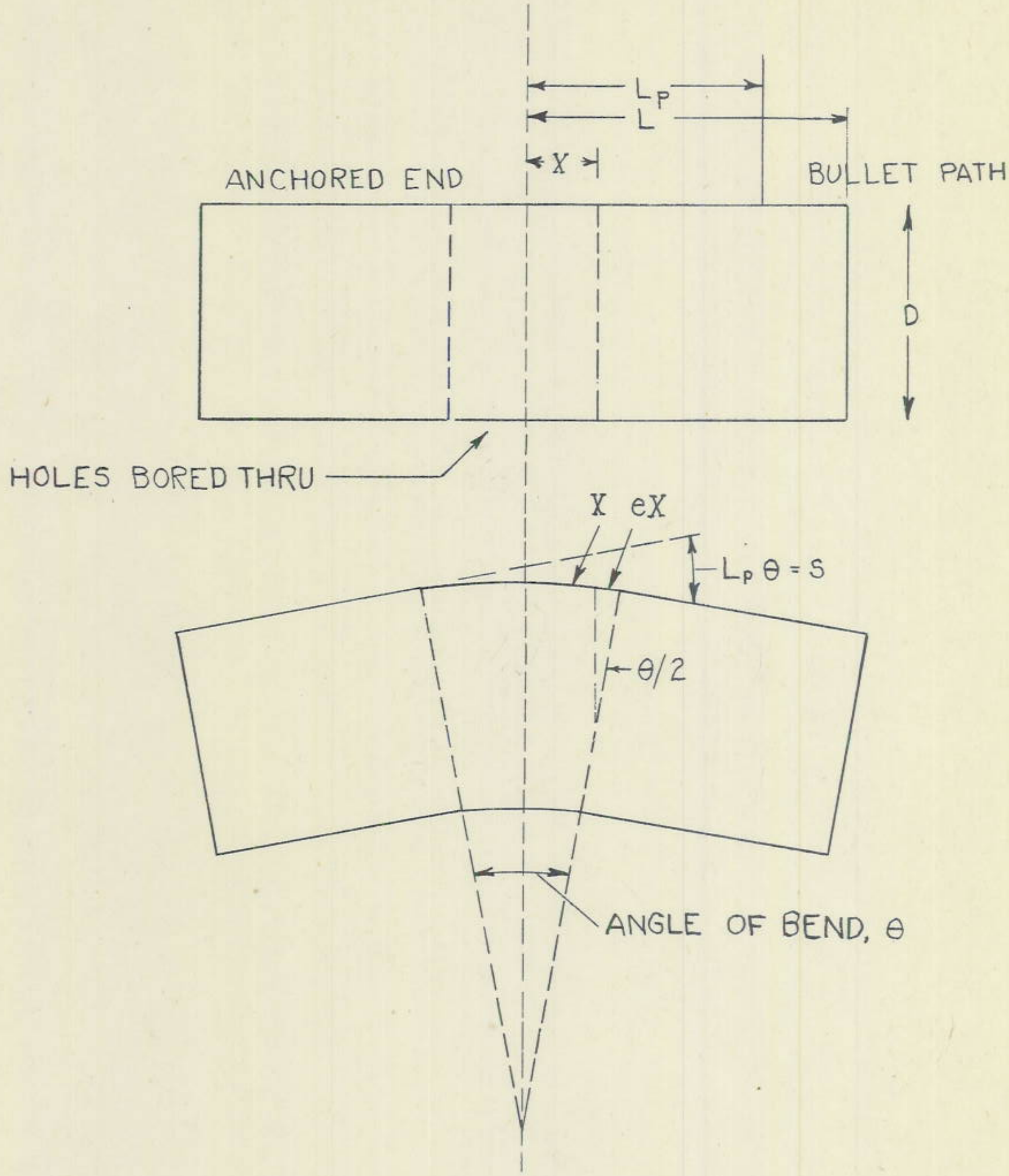

L P
L
X
ANCHORED END
BULLET PATH
D
HOLES BORED THRU
X eX
Lp θ = S
θ/2
ANGLE OF BEND, θ

FIG. 17

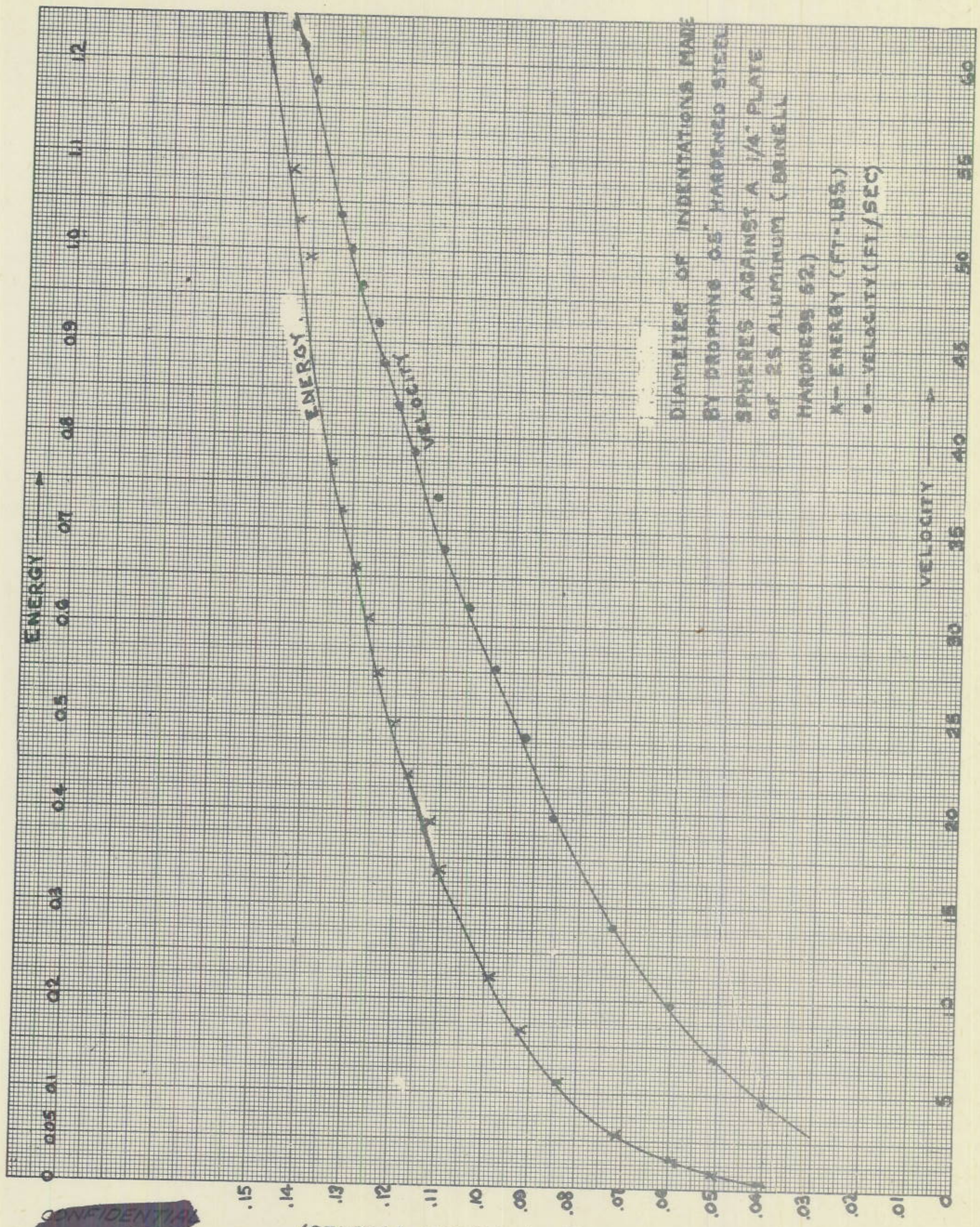

FIG. 18

DECLASSIFIED

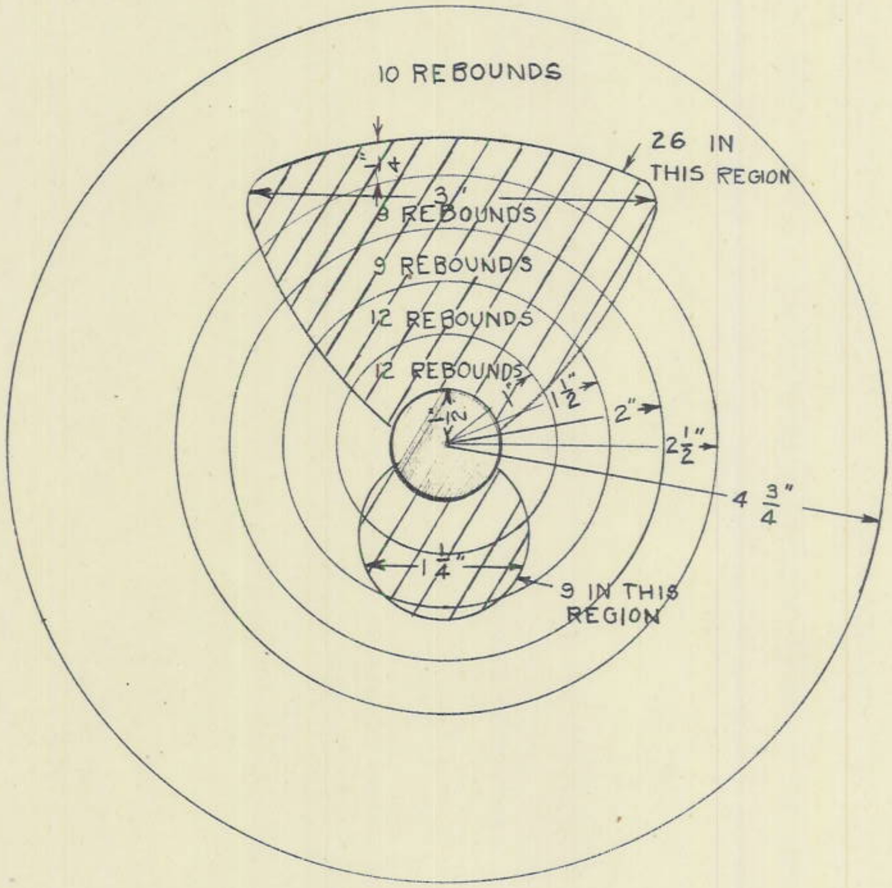

DISTRIBUTION OF INDENTATIONS MADE BY 0.5" SPHERES REBOUNDING TO A PLATE OF 2S ALUMINUM. - 52 B.H.N. $8\frac{1}{2}$" FROM SPECIMEN TO PLATE

FIG. 19

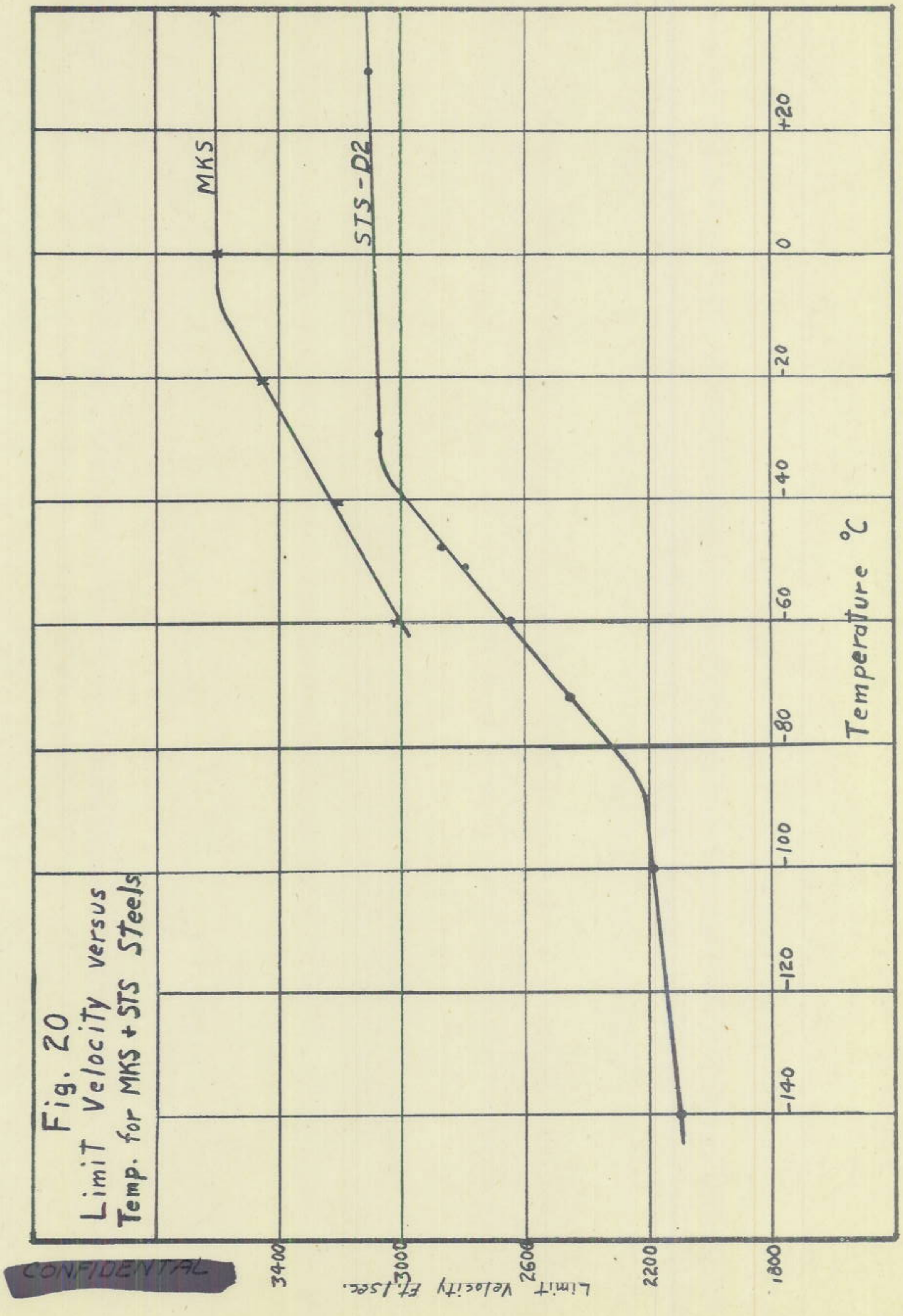

Fig. 20
Limit Velocity versus
Temp. for MKS + STS Steels